Antiviral Research 164 (2019) 106–122

Contents lists available at ScienceDirect

Antiviral Research

journal homepage: www.elsevier.com/locate/antiviral

Proteolytic cleavage of host proteins by the Group IV viral proteases of Venezuelan equine encephalitis virus and Zika virus

Elaine M. Morazzani[a], Jaimee R. Compton[d], Dagmar H. Leary[d], Angela V. Berry[b], Xin Hu[c], Juan J. Marugan[c], Pamela J. Glass[a], Patricia M. Legler[d,*]

[a] United States Army Medical Research Institute of Infectious Diseases, Frederick, MD 21702, USA
[b] Hampton University School of Pharmacy, Hampton, VA, USA
[c] NIH Chemical Genomics Center, National Center for Advancing Translational Sciences, Rockville, MD 20850, USA
[d] Center for Bio/molecular Science and Engineering, U.S. Naval Research Laboratory, Washington, DC 20375, USA

ARTICLE INFO

Keywords:
VEEV
Alphavirus
nsP2 protease
Protease inhibitors
Host protein substrates
Innate immune response
Evasion
Interferon antagonism
Host-pathogen interactions
Co-translational silencing
Post-translational silencing
Antiviral drug target
Zika virus
Microcephaly

ABSTRACT

The alphaviral nonstructural protein 2 (nsP2) cysteine proteases (EC 3.4.22.-) are essential for the proteolytic processing of the nonstructural (ns) polyprotein and are validated drug targets. A common secondary role of these proteases is to antagonize the effects of interferon (IFN). After delineating the cleavage site motif of the Venezuelan equine encephalitis virus (VEEV) nsP2 cysteine protease, we searched the human genome to identify host protein substrates. Here we identify a new host substrate of the VEEV nsP2 protease, human TRIM14, a component of the mitochondrial antiviral-signaling protein (MAVS) signalosome. Short stretches of homologous host-pathogen protein sequences (SSHHPS) are present in the nonstructural polyprotein and TRIM14. A 25-residue cyan-yellow fluorescent protein TRIM14 substrate was cleaved *in vitro* by the VEEV nsP2 protease and the cleavage site was confirmed by tandem mass spectrometry. A TRIM14 cleavage product also was found in VEEV-infected cell lysates. At least ten other Group IV (+)ssRNA viral proteases have been shown to cleave host proteins involved in generating the innate immune responses against viruses, suggesting that the integration of these short host protein sequences into the viral protease cleavage sites may represent an embedded mechanism of IFN antagonism. This interference mechanism shows several parallels with those of CRISPR/Cas9 and RNAi/RISC, but with a protease recognizing a protein sequence common to both the host and pathogen. The short host sequences embedded within the viral genome appear to be analogous to the short phage sequences found in a host's CRISPR spacer sequences. To test this algorithm, we applied it to another Group IV virus, Zika virus (ZIKV), and identified cleavage sites within human SFRP1 (secreted frizzled related protein 1), a retinal G_s alpha subunit, NT5M, and Forkhead box protein G1 (FOXG1) *in vitro*. Proteolytic cleavage of these proteins suggests a possible link between the protease and the virus-induced phenotype of ZIKV. The algorithm may have value for selecting cell lines and animal models that recapitulate virus-induced phenotypes, predicting host-range and susceptibility, selecting oncolytic viruses, identifying biomarkers, and de-risking live virus vaccines. Inhibitors of the proteases that utilize this mechanism may both inhibit viral replication and alleviate suppression of the innate immune responses.

1. Introduction

Group IV viruses are positive sense single stranded RNA ((+)ssRNA) viruses. Several new and emerging pathogens can be found among the group which includes the *Coronaviridae*, *Picornaviridae*, and *Flaviviridae* families among others. Alphaviruses belong to the *Togaviridae* family of Group IV. These viruses utilize multiple redundant mechanisms to antagonize the interferon (IFN) response (Hollidge et al., 2011), but also have limitations with regards to the size of their genomes. To evade the innate immune responses, alphaviruses shut off host cell transcription and translation, typically within hours post-infection (Garmashova et al., 2006, 2007a; Simmons et al., 2009) to prevent the expression of IFN-stimulated genes (ISG) that can inhibit their replication (Simmons et al., 2009; Schoggins and Rice, 2011; Zhang et al., 2007; Fros and Pijlman, 2016).

The nonstructural proteins (nsPs) play essential roles in replication, but also can play secondary roles, typically in IFN-antagonism. For example, the papain-like protease of SARS is also a deubiquitinase

* Corresponding author. 4555 Overlook Ave., SW, Washington, DC 20375, USA.
E-mail address: Patricia.legler@nrl.navy.mil (P.M. Legler).

https://doi.org/10.1016/j.antiviral.2019.02.001
Received 13 October 2018; Received in revised form 13 January 2019; Accepted 1 February 2019
Available online 10 February 2019

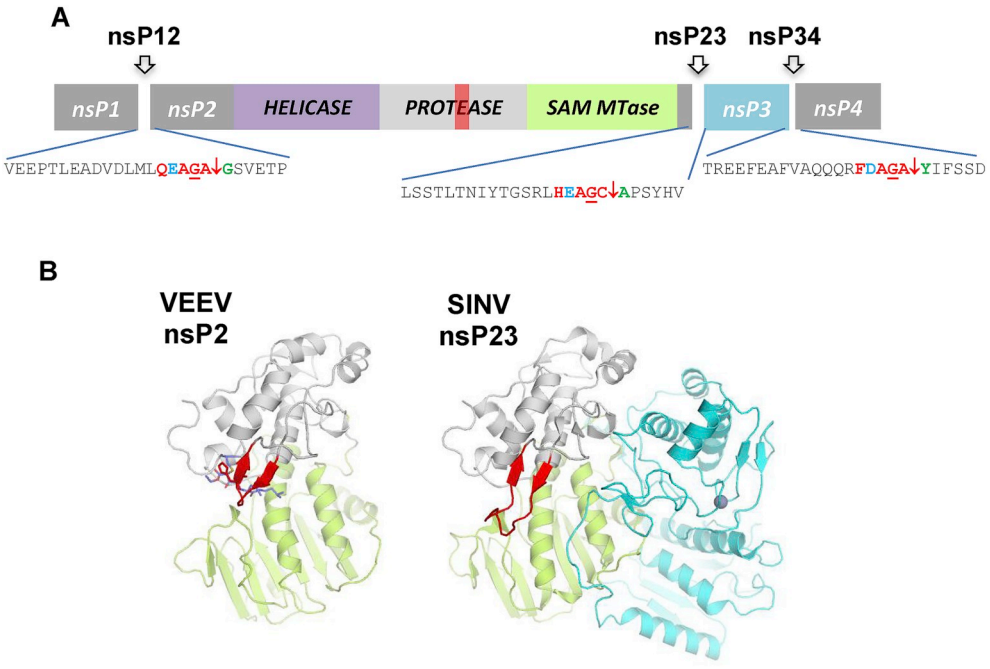

Fig. 1. Organization of the alphaviral nonstructural polyprotein. (A) The nsP2 contains an N-terminal region, a helicase (purple), a papain-like cysteine protease (gray), and SAM MTase (lime). The nsP2 cysteine protease cleaves the polyprotein to produce nsP1, nsP2, nsP3, and nsP4. **(B)** Crystal structure (PDB 5EZS) (Hu et al., 2016) of the nsP2 cysteine protease inhibited with E64d shows that the protease and SAM MTase domains pack together. The peptide-like E64d inhibitor binds beneath the β-hairpin (red) at the interface of these two domains. The structure of the pre-cleavage nsP23 complex (PDB 4GUA) shows the packing of the nsP3 domain (cyan) (Shin et al., 2012). **(C)** Sequence alignment of the human TRIM14 protein with the alphaviral nsP cleavage sites. The P4 residue is shown in blue. The highly conserved cleavage site motifs are shown in red and green. The New World alphaviruses and TRIM14 share the QEAGA↓G sequence.

(Ratia et al., 2008; Compton et al., 2017). The role of the nsPs in IFN-antagonism can be either enzymatic or non-enzymatic (e.g., binding). The nonstructural proteins of alphaviruses are translated as a single polyprotein (nsP1234) which is then processed by the nsP2 protease to yield four separate proteins (nsP1, nsP2, nsP3, nsP4). This is an essential step during viral replication (Fig. 1A). The nsP2 protease is a validated drug target (validated by both deletion and mutation of the nucleophilic cysteine) (Hardy and Strauss, 1989; Strauss et al., 1992; Ding and Schlesinger, 1989). The nsP2 of alphaviruses contains an N-terminal domain, a helicase, a papain-like protease, and an S-adenosyl-L-methionine-dependent RNA methyltransferase (SAM MTase) domain (Fig. 1). The nsP2 of Old World alphaviruses (Sindbis virus(SINV), Semliki Forest virus (SFV), and Chikungunya (CHIKV)), can inhibit transcription in a manner that is independent of its protease activity, but reliant on its helicase activity (Akhrymuk et al., 2012). These nsP2 proteins induce the rapid degradation of Rpb1, a catalytic subunit of the RNA polymerase II complex, through nsP2-mediated ubiquitination (Akhrymuk et al., 2012). Transcriptional shut-off mechanisms are known to differ for Old and New World alphaviruses (Garmashova et al., 2007a). In cells infected with the New World alphavirus, VEEV,

transcriptional shutoff is mediated by a ~35-residue sequence at the N-terminus of the capsid protein; the capsid is thought to partially obstruct the nuclear pore complex to block host mRNA export (Garmashova et al., 2007b; Atasheva et al., 2010). While these viruses can effectively counter the innate immune responses using these shutoff mechanisms, intrinsic immune factors pose additional challenges since these proteins are present prior to viral infection, and sufficient quantities of viral proteins (e.g., capsid) may not be present to override their effects early in infection. Catalytic amounts of the viral enzymes may thus be important for establishing infection.

The (+)ssRNA genomes of Group IV viruses are essentially mRNA that can be translated immediately after entry into the cell, preceding genome replication events (Fata et al., 2002). We hypothesized that the alphaviral protease cleavage sites may share homology with human proteins and that the virus may use these short stretches of host sequences in its cleavage sites as an embedded mechanism of IFN-antagonism that can be propagated generationally. We previously characterized the VEEV nsP2 substrate specificities using kinetic, mutational, and structural studies (Compton et al., 2017; Hu et al., 2016). Here, we have examined potential host protein targets of the nsP2 protease by searching the human genome for proteins sharing sequence identity with the nsP12, nsP23, and nsP34 cleavage site sequence motifs. We identified one human protein, TRIM14 (also known as Pub (Hirose et al., 2003)), sharing six consecutive residues with an alphaviral nsP12 cleavage site using BLAST.

TRIM14 is a tripartite motif (TRIM) protein and was recently shown to function as an adaptor protein in the MAVS signalosome (Nenasheva et al., 2015; Zhou et al., 2014). Stable overexpression of TRIM14 has been shown to inhibit alphaviral replication (SINV) by 3–4 logs 24 h post-infection (Nenasheva et al., 2015). TRIM14 overexpression also increases the transcription of IFNs and interferon-stimulated genes (ISG) (Nenasheva et al., 2015). The viral proteases' ability to cleave a host protein involved in the production of the innate immune responses appears to be a common antagonistic mechanism used by this and other Group IV viral proteases. To test this viral "search and delete" algorithm, we identified four host protein sequences that can be cleaved by the Zika ns2B/ns3 protease. We discuss the similarities of this co- or post-translational silencing mechanism with those of CRISPR/Cas9 and RNAi/RISC and its potential applications. Many variations of these silencing mechanisms have been proposed; however, a protein-version has not. The algorithm may be a useful bioinformatics tool (Ibrahim et al., 2018) to predict host-pathogen interactions specifically with Group IV viruses. An abstract of this work has been published (Morazzani et al., 2017).

2. Materials & methods

2.1. Materials

RIPA buffer, Halt™ Protease Inhibitor Cocktail and all general chemicals were purchased from Fisher Scientific (Waltham, MA). Plasmid constructs were synthesized by Genscript USA, Inc. (Piscataway, NJ). BugBuster™ and IPTG (#420291) were purchased from EMD Millipore (Billerica, MA). Column resins and PD-10 gel filtration columns were purchased from G. E. Healthcare (Pittsburgh, PA). Ethylenediaminetetraacetic acid (EDTA)-free Protease inhibitor tablets were from Roche, Inc. Black half-area Corning 3993 non-binding surface 96-well plates were from Corning Inc. (Corning, NY). Pierce Precise Tris-HEPES acrylamide gels (8–16% gradient) and BupH Tris-HEPES SDS-PAGE running buffer were from Thermo Scientific (Rockford, IL). The anti-TRIM14 antibody HPA053217 was from Sigma (St. Louis, MO) and the anti-TRIM14 antibody ARP34737_P050 was from Aviva Systems Biology (San Diego, CA). The anti-actin antibody was from Abcam Inc. (Cambridge, MA).

2.2. Plasmid constructs of FRET substrates

A pET-15b plasmid (Novagen Inc., Madison, WI) encoding cyan fluorescent protein (CFP), an nsP2 protease cleavage site motif, A**G**(A/C/R)↓(G/Y/A), and yellow fluorescent protein (YFP) in between the *Nde*I and *Xho*I cut sites was synthesized by Genscript Inc. (Piscataway, NJ). An N-terminal hexa-histidine tag preceded a thrombin cleavage site. Protein sequences are included in the Suppl. Info. Twelve CFP-YFP constructs were used: V12 which contains 25-residues of the VEEV nsP12 cleavage site; V34 which contains 25-resdiues of the VEEV nsP34 cleavage site; S12 which contains 25-residues of the SFV nsP12 cleavage site; three TRIM14 substrates containing 25-, 22-, or 19-residues of human TRIM14; six substrates containing sequences from SFRP1, SFRP2, SFRP4, Gs Galpha, NT5M, and FOXG1.

2.3. Plasmid constructs of the nsP2 cysteine Protease-SAM MTase

The VEEV nsP2 cysteine protease and SAM MTase domains (residues 457-792) were encoded on a single polypeptide and were fused to thioredoxin (Trx) and a hexa-histidine tag with a thrombin cleavage site in a pET-32a vector (Novagen, Inc.). Similar constructs were made for the Eastern (EEEV) and Western (WEEV) equine encephalitis virus nsP2 cysteine protease-SAM MTase proteins. The His-tag in the VEEV construct was associated with thioredoxin and both were removed by thrombin cleavage.

The nsP2 cysteine protease-SAM MTase of CHIKV in a modified pMCSG9 vector was kindly provided by Dr. Jonah Cheung at the New York Structural Biology Center (Cheung et al., 2011). The CHIKV protease/SAM MTase was fused to a decahistidine-tagged maltose-binding-protein (MBP) at the N-terminus that could be cleaved using TEV protease.

2.4. Expression & purification of the nsP2 cysteine proteases

To ensure purification of the reduced state of the VEEV nsP2 cysteine protease, we used an nsP2-Trx fusion protein (Suppl. Info.) (Hu et al., 2016). BL-21(DE3) pLysS *E. coli* were transformed with the Trx-VEEV-nsP2 plasmid. Luria Bertani (LB) media (3–6 L) containing 50 μg/mL ampicillin and 25 μg/mL chloramphenicol was inoculated and grown to an OD_{600} of approximately 1.0 and induced with 0.5 mM IPTG overnight at 17 °C. Cells were pelleted and lysed with lysis buffer (50 mM Tris pH 7.6, 500 mM NaCl, 35% BugBuster, 5% glycerol, 2 mM β-mercaptoethanol (BME), 25 U of DNase, 0.3 mg/mL lysozyme) and sonicated ten times for 15 s intervals in an ice bath. Lysates were clarified by centrifugation at 20,000 × *g* for 30 min and loaded onto a nickel column equilibrated with 50 mM Tris pH 7.6, 500 mM NaCl, 2 mM BME, 5% glycerol. The column was washed with the same buffer containing 60 mM imidazole. Protein was eluted using the same buffer containing 300 mM imidazole. Protein was dialyzed with thrombin (overnight at 4 °C) against 50 mM Tris pH 7.6, 250 mM NaCl, 5 mM dithiothreitol (DTT), 1 mM EDTA, 5% glycerol, and then diluted 1:3 with Buffer A (50 mM Tris pH 7.6, 5% glycerol, 5 mM DTT) and loaded onto an SP-Sepharose column equilibrated with Buffer A. Protein was eluted using a salt gradient (0–1.25 M NaCl) and then concentrated, flash frozen in liquid nitrogen and stored at −80 °C or at −20 °C in buffer containing 50% glycerol. The buffer was exchanged to the corresponding assay buffer (50 mM HEPES pH 7.0) prior to kinetic experiments using PD-10 columns. The EEEV and WEEV nsP2 cysteine proteases were expressed and purified using a similar protocol with an additional Q-Sepharose column purification step prior to the SP-Sepharose column. The CHIKV nsP2 protease was purified using a similar method (Hu et al., 2016); the His-tag and MBP were removed.

2.5. Expression & purification of the ZIKV ns2B/ns3 protease

The pet15 plasmid encoding the ZIKV ns2B/ns3 protease was a kind

gift of Dr. Rolf Hilgenfeld and Dr. Jian Lei (Univ. Lübeck, Germany) (Lei et al., 2016). The construct contains two conservative substitutions that are distant from the active site, C1080S and C1143S. The protease was purified using the same procedure as was used for the VEEV nsP2 protease.

2.6. Expression & purification of FRET protein substrates and CFP-PRY/SPRY substrate

BL-21(DE3) *E. coli* were transformed with the plasmids encoding the substrates. LB/Amp (1.5–3.0 L) was inoculated and grown to an OD_{600} of approximately 1.0 and induced with 0.5 mM IPTG overnight with shaking at 17 °C. Cells were pelleted by centrifugation, lysed with lysis buffer (50 mM Tris pH 7.6, 500 mM NaCl, 35% BugBuster, 25 U DNase, 0.3 mg/mL lysozyme, 1 EDTA-free protease inhibitor tablet), and briefly sonicated for 1 min in an ice bath. Lysates were clarified by centrifugation (20,500 × *g* for 30 min at 4 °C) and loaded onto a nickel column equilibrated with 50 mM Tris pH 7.6, 500 mM NaCl. The column was washed with the same buffer after loading, and with 10–20 column volumes of buffer containing 60 mM imidazole until the A_{280} returned to baseline. The protein was eluted with the same buffer containing 300 mM imidazole. The protein was dialyzed against 50 mM Tris pH 7.6, 150 mM NaCl overnight at 4 °C with 50 U thrombin. The His-tag was removed by re-running the protein on a nickel column and collecting the flow-through. The protein then was dialyzed against 50 mM Tris pH 7.6, 5 mM EDTA, 250 mM NaCl (overnight at 4 °C), followed by dialysis against 50 mM Tris pH 7.6 (2 h). For substrates containing cysteine, 2 mM BME or DTT was included in the buffers. Protein was loaded onto a Q-Sepharose column equilibrated with 50 mM Tris pH 7.6 and eluted with a salt gradient (0–1 M NaCl). Most substrates were produced in high yield (typical yields were 60–80 mg per liter of media) and could be concentrated readily to 9.0–10.5 mg/mL. The substrates were used for continuous and discontinuous assays. Similar substrates have been used to study other proteases (Ruge et al., 2011).

For expression of the PRY/SPRY domain of TRIM14, a homology model was used to isolate the globular domain (Suppl. Info.). The domain was fused to an N-terminal His-tagged CFP (CFP-PRY/SPRY) and expressed in *E. coli* Shuffle pLysY (#C3030, New England Biolabs Inc., Ipswich, MA) to enable disulfide bond formation. Cells were lysed in the presence of protease inhibitors (2 tablets per 100 mL, Pierce™ #A32955, Grand Island, NY) in 50 mM Tris pH 7.6, 500 mM NaCl, 35% BugBuster, 5 mg DNase, and 30 mg lysozyme. The lysate was sonicated for 1 min and clarified by centrifugation (20,500 × *g*, 30 min, 4 °C). Protein was purified by nickel column (50 mM Tris pH 7.6, 500 mM NaCl), washed with buffer containing 60 mM imidazole, and eluted with a gradient (60–300 mM imidazole). For cleavage assays, the CFP-PRY/SPRY protein was buffer exchanged into 50 mM HEPES pH 7.4, 150 mM NaCl. The VEEV nsP2 protease was briefly treated with a serine protease inhibitor (AEBSF, 1 mg/mL) for 7 min at room temperature (RT) and the inhibitor was removed by a PD-10 column (50 mM Tris pH 7.6, 500 mM NaCl, 5 mM DTT, 5% glycerol). CFP-PRY/SPRY cleavage reactions were setup in the same buffer and contained 2 μM substrate and 2 μM enzyme. The substrate was digested overnight at room temperature for 18 h and reactions were stopped with an equal volume of 2× Laemelli buffer containing BME (355 mM). Cleavage products were separated by SDS-PAGE and blotted onto nitrocellulose. The cut products were detected using an anti-Histag antibody (1:2000, Novagen Inc., #70796) or anti-TRIM14 antibody (1:1000 Aviva, ARP34737_P050). This TRIM14 antibody was raised to an immunogen sequence (LVEAVESTLQTPLDIRLKESINCQLSDPSSTKPGTLLKTSPSPERSLLLK) that is present in the predicted PRY/SPRY domain and precedes the QEAGA↓G sequence.

2.7. Continuous FRET assay

For measurement of steady state kinetic parameters the method described by Ruge et al. was followed (Ruge et al., 2011). Cleavage of the YFP/CFP FRET substrates was monitored continuously at room temperature (23 ± 3 °C) using excitation/emission wavelengths of 434/470 nm and 434/527 nm to calculate emission ratios and a SpectraMax M5 plate reader from Molecular Devices, LLC. (San Jose, CA). The substrate was buffer-exchanged into 50 mM HEPES pH 7.0. Enzyme concentrations of ≤1 μM and a substrate concentration range of 10–140 μM (8 different concentrations) were used to measure steady state kinetic parameters. Data were collected in triplicate (50 μL reaction volumes) in half-area black low binding surface 96-well plates from Corning, Inc. (Corning 3993). After the reads were completed, the plates were sealed with film and allowed to digest overnight at room temperature (23 ± 3 °C). Final emission ratios were read the next day. The fraction of substrate cleaved, f, was calculated from the emission ratios at each time point using the following equation:

$$f = \frac{\left[\frac{\left(\frac{ex434}{em527}\right)}{\left(\frac{ex434}{em470}\right)} - r_{uncut}\right]}{(r_{cut} - r_{uncut})}$$

The nmols of substrate cleaved at each time point were calculated by multiplying f by the nmols of substrate at t = 0 (S_o). The value of r_{uncut} corresponds to the emission ratio measured in the absence of enzyme and the value of r_{cut} is the emission ratio measured when the substrate was fully cleaved. Initial velocities were calculated at each [S] concentration from the linear range (f ≤ 20%). Plots of time vs. nmols were linearly fit for each [S] concentration and v_o was obtained from the slopes of the lines. Rates of spontaneous hydrolysis were measured in the absence of enzyme and were subtracted from the enzyme catalyzed rates. Data were fit to the Michaelis-Menten equation, $v_o = (V_{max}*[S])/(K_m + [S])$ using GraFit (Erithricus Software Ltd., Surrey, UK).

2.8. Discontinuous gel-based assay

Reaction mixtures (5 μM nsP2-Trx, 50 μM FRET substrate, 50 mM HEPES pH 7.0, 150 mM NaCl) were incubated overnight (~18 h) at room temperature (23 ± 3 °C). The reactions were run until > 90% of the substrate was cleaved by the enzyme. Reactions were stopped by mixing with Laemelli buffer (1:1) and heating the samples for 3 min at ≥70 °C. Cleavage products (10 μL) were separated by SDS-PAGE. The calculated molecular weight (MW) of the uncut TRIM14 FRET substrate containing a 25 amino acid cleavage sequence was 56.7 kDa, and 29.2 kDa and 27.5 kDa for the cut CFP and YFP products. The MW of the enzyme for the Trx-His-tagged enzyme was 52.2 kDa, and 38.3 kDa for the Tag-free enzyme. The bands were well separated in 12% gels or 8–16% gradient gels and boiling of the samples was required to achieve the sharp banding pattern. Densitometry was done using the BioRad Gel Dock Imager software (BioRad Inc., Hercules, CA).

2.9. Mass spectrometry

Gel bands were washed with 250 mM ammonium bicarbonate in 50% acetonitrile (ACN) until completely destained. Bands were then cut into small cubes and dehydrated by 100% ACN. Modified porcine trypsin solution (Promega Inc., Madison, WI, #V511) in 50 mM ammonium bicarbonate was added to gel cubes and proteins were in-gel digested overnight. The resulting peptides were extracted from the gel pieces by sonication in 2% formic acid (FA) in 60% ACN. The extracts were then collected and this step was repeated three more times. A final gel dehydration step (i.e., sonication with 100% ACN) was used to minimize peptide loss. Peptide digests corresponding to the same band were combined and concentrated via speed-vac.

Concentrated in-gel digests were reconstituted in 0.1% FA and 5% ACN and injected onto a reverse phase column (C18, Michrom Magic – C18AQ-5μ 200 Å 0.1 × 150 mm) using a Tempo MDLC system (AB Sciex, Foster City, CA) coupled to a quadrupole-time of flight (TOF) MS/MS Q-Star Elite mass spectrometer (MS) (AB Sciex). Peptides were loaded onto the column using 98% solvent A (5% ACN, 0.1% FA in water) and 2% solvent B (95% ACN, 0.1% FA in water) for 30 min and separated by a 130 min linear gradient of increasing solvent B by 0.37%/min to a final concentration of 50%. MS and MS/MS peptide spectra were acquired using information dependent acquisition (IDA). A mass range of 350–1600 Da was monitored in TOF MS scan. The three most abundant precursor ions from TOF MS scans with an intensity > 20 counts per second were submitted for MS/MS analyses. Former target ions were excluded from MS/MS submission for 15 s. MS data were acquired using Analyst QS (AB Sciex). Tandem mass spectra were extracted by mascot.dll and analyzed using Mascot (Matrix Science, London, UK; Mascot Server version 2.4.1). Mascot was set up to search three in-house databases: **1:** contaminants 20120713 (247 sequences; 128,130 residues); **2:** cRAP 20121128 (112 sequences; 37,418 residues); and **3:** VEEV database (6 sequences; 1,980 residues). Common contaminants were included in the first two databases while the complete VEEV protease, Trx, complete sequence of CFP-TRIM14-YFP, as well as its predicted N-terminal and C-terminal sequences as produced by the VEEV protease were included in the third database. Data were analyzed assuming the digestion was semitryptic (at least one peptide terminal was R or K) and allowing for 3 miscleavages. Fragment ion mass tolerance was set to 0.20 Da and a parent ion tolerance to 0.20 Da. Deamidation of asparagine and glutamine, oxidation of methionine were set as variable modifications. After identification by Mascot, the spectra of resulting N-terminal and C-terminal peptides of TRIM14 products from VEEV proteolysis (HYWEVDVQEAGA and GWWVGAMVSK) were inspected manually in the raw acquired data, and the resulting singly charged fragments were manually annotated.

2.10. Western blotting

Cells were lysed in RIPA buffer containing Halt Protease Inhibitor Cocktail at a 2× final concentration. Lysates were separated in a 10% NuPAGE Bis-Tris gel and electroblotted onto a nitrocellulose membrane using the iBlot system (Invitrogen Inc., Grand Island, NY). Following protein transfer, blots were blocked in 1× phosphate-buffered saline (PBS) containing 0.05% Tween-20 and 5% dry milk and incubated at 4 °C overnight. Protein-specific primary antibodies (Ab) were diluted in blocking buffer and incubated at RT for 2 h. Following incubation, blots were washed 3 times with PBS containing 0.05% Tween-20 (PBST). After washing, blots were incubated with corresponding secondary antibody at RT for 1 h then washed 3 times with PBST. For protein detection, blots were treated with SuperSignal™ West Pico Chemiluminescent Substrate (Thermo Sci. Inc., Waltham, MA) and imaged using BioRad imaging software. TRIM14 protein was detected using a polyclonal anti-TRIM14 Ab (1:500, HPA053217) followed by goat anti-rabbit horseradish peroxidase (HRP, 1:500) secondary Ab. Actin protein was detected using anti-actin Ab (1:5000) followed by goat anti-mouse HRP (1:5000) secondary Ab.

A549 cells (adenocarcinoma human alveolar basal epithelial cells, ATCC) were used for viral infection studies. Infected A549 cell lysates collected at 6 and 24 h post-infection (10 μg/lane) were separated in a 10% NuPAGE Bis-Tris gel and transferred onto a nitrocellulose membrane. TRIM14, TRIM14 cleavage product (CP), and α-actin were detected by Western blot analysis using protein specific antibodies. Recombinant Human TRIM14 protein was used as control. The VEEV Trinidad, EEEV FL93-939, WEEV CBA87, and CHIKV AF15561 viruses were used.

To test the effects of a previously identified VEEV nsP2 cysteine protease inhibitor (Campos-Gomez et al., 2016), CA074 methylester (CA074me), A549 cells were treated with CA074me and infected at a multiplicity of infection equal to 10 with VEEV or CHIKV. After incubation of virus with cells for 1 h, cell monolayers were washed twice with medium to remove residual virus. Complete medium containing CA074me (50, 100, 200 μM) was added and the cells were incubated at 37 °C, 5% CO_2. 18–24 h post-infection, supernatants and cell lysates were collected for analysis by Western blot.

The specificity of the polyclonal rabbit Sigma Prestige™ anti-TRIM14 antibody (HPA053217) has already been analyzed and is available online (Fagerberg et al., 2014; Uhlen et al., 2015). The HPA053217 antibody had been raised using the immunogen sequence (HIDNITQIEDATEKLKANAESSKTWLKGKFTELRLLLDEEEALAKKFIDKNTQLTLQVYREQADSCREQLDIMNDLS). This N-terminal sequence is common to full-length TRIM14 and the α- and β-isoforms of TRIM14. The sequence precedes the ubiquitination site.

For expression of recombinant full-length His_6-tagged TRIM14 (rTRIM14) and the VEEV nsP2 in cells pcDNA3.4 plasmids containing the sequences were co-transfected into A549 cells (Sigma) using Lipofectamine 3000 (Invitrogen Inc.). Cells were collected at 6, 24, 48 h post-transfection and lysed by sonication (10 s) in MPER containing 10 mM DTT, 1% NP-40, 5 mM EDTA, and 4 mg/mL AEBSF (4-(2-aminoethyl)benezenesulfonyl fluoride). Blots were probed with the Sigma HPA053217 anti-TRIM14 antibody (1:500) and mouse anti-Histag antibody (1:1000, Abcam ab18184).

2.11. Modeling of substrate binding interaction

The binding models of substrates including VEEV P12, P23, P34 and TRIM14 were predicted with an ensemble-docking protocol using the AutoDock program (Morris et al., 2009). Multiple conformations of the VEEV nsP2 structure (PDB 2HWK) and the CHIKV nsP2 (PDB 3TRK) were obtained from MD simulations and cluster analysis. The active site of the protein was defined by a grid of 70 × 70 x 70 points with a grid spacing of 0.375 Å centered at the catalytic residue Cys-477. The Lamarckian Genetic Algorithm (LGA) was applied with 50 runs and the best pose with the most favorable binding free energy was selected. MD simulations were performed for the predicted substrate binding models using the AMBER 12 package and the ff99SB force field. The solvated systems were subjected to a thorough energy minimization prior to MD simulations. Periodic boundary conditions were applied to simulate a continuous system. The particle mesh Ewald (PME) method was employed to calculate the long-range electrostatic interactions. The simulated system was first subjected to a gradual temperature increase from 0 K to 300 K over 100 ps, and then equilibrated for 500 ps at 300 K, followed by production runs of 2-ns length in total. The binding free energies were calculated using the MM-PBSA method. Decomposition of the calculated binding free energies was performed using the same MM-PBSA module in AMBER 12 package.

3. Results

3.1. VEEV nsP2 cysteine protease cleaves human TRIM14 at Ala-333

We previously identified the sequences N- and C-terminal to the scissile bond that were recognized by the VEEV nsP2 cysteine protease using a set of variable length substrates and found that 25-residue substrates containing P19-P6' (Schechter and Berger nomenclature (Schechter and Berger, 1967)) produced the lowest K_m values (Hu et al., 2016). A BLAST search (Altschul et al., 1990) using the nsP2 cleavage sites and the human genome uncovered one protein, TRIM14, which had a high level of sequence identity to the VEEV nsP12 cleavage site (Fig. 1C). The nsP12 cleavage site sequence QEAGA↓G is highly conserved among the more virulent New World alphaviruses, VEEV/EEEV/WEEV, but not in the Old World alphaviruses such as SINV, SFV, and CHIKV. Some overlap in substrate specificities has been observed for the VEEV and CHIKV nsP2 proteases; for example, both are able to cleave the Old World SFV nsP12 cleavage site (Hu et al., 2016; Zhang

A

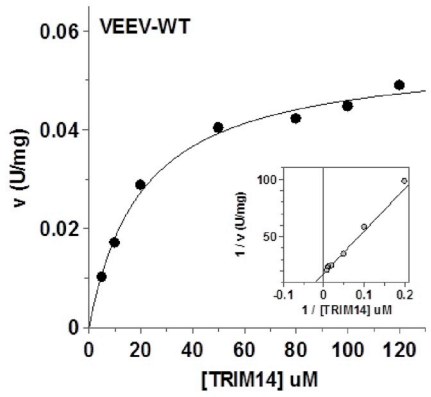

B

Substrate		Length	V_{max} (U/mg)	K_m (μM)
CFP-V12-YFP	VEEPTLEADVDLMLQEAGA↓GSVETP	25	0.059 ± 0.003	12 ± 3
CFP-V34-YFP	TREEFEAFVAQQQRFDAGA↓YIFSSD	25	0.089 ± 0.005	21 ± 4
CFP-TRIM14-YFP	DCFATGRHYWEVDVQEAGA↓GWWVGA	25	0.056 ± 0.002	21 ± 2
	ATGRHYWEVDVQEAGA↓GWWVGA	22	0.0080 ± 0.0003	26 ± 4
	RHYWEVDVQEAGA↓GWWVGA	19	0.012 ± 0.002	50 ± 20

C

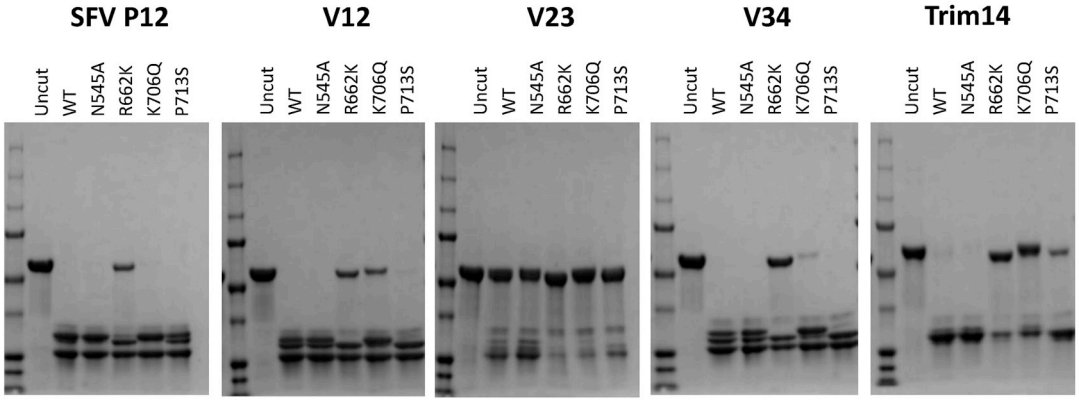

Fig. 2. ***In vitro*** **assays demonstrating the cleavage of TRIM14 by the VEEV nsP2 cysteine protease. (A)** Measurement of the VEEV nsP2 cysteine protease steady state kinetic parameters for the 25-residue CFP-TRIM14-YFP substrate measured at R.T. in 50 mM HEPES pH 7.0 for 30 min. The K_m and V_{max} were comparable to those measured using similar substrates containing the VEEV nsP12 or nsP34 cleavage sites. **(B)** Steady state kinetic parameters for the VEEV nsP2 cysteine protease and substrates containing either the natural viral cleavage sequences at each of the junctions or the variable length TRIM14 sequences. All were measured in 50 mM HEPES pH 7.0 and R.T. **(C)** Effects of site-directed mutagenesis on cleavage of CFP-YFP substrates containing the SFV nsP12 cleavage site, the VEEV nsP12, nsP23, nsP34 cleavage sites, and the TRIM14 sequence. Cleavage reactions were run in 1× PBS pH 7.4 and 5 mM DTT and were incubated for 19 h at R.T. using 30 μM substrate and 2.2 μM enzyme. Subtle changes in MW (~2 kDa) and additional cleavage product bands for some of the enzyme variants are likely due to trace amounts of residual thrombin from the purification. A C477A nsP2 protease variant was included as a control in the Suppl. Info.

et al., 2009).

Using a CFP-YFP substrate containing 25-amino acids of the human TRIM14 protein, the purified VEEV nsP2 protease was found to cleave the TRIM14 substrate (Fig. 2). Cleavage was confirmed by SDS-PAGE; the effects of site-directed mutagenesis on the cleavage of the TRIM14 substrate were similar to those observed for the substrate containing the VEEV nsP12 cleavage site, suggesting similar enzyme and substrate contacts (Fig. 2C). For the VEEV nsP2 protease, the cleavage site in the CFP-YFP substrate was confirmed by tandem mass spectrometry (Fig. 3, Suppl. Fig. S1), and cleavage occurred at the expected site at QEAGA↓G. The tryptic peptides of both parts of the substrate were identified.

3.1.1. Steady state kinetic parameters for the VEEV nsP2 cysteine protease and TRIM14 substrate

Steady state kinetic parameters were measured to determine if the K_m and V_{max} measured with the TRIM14 25-residue substrate were similar to those obtained with substrates containing the viral cleavage sites (Fig. 2A and B). The K_m and V_{max} obtained with the wild type (WT) VEEV nsP2 protease and the TRIM14 substrate were comparable to those obtained with the nsP12 and nsP34 substrates. The length of the TRIM14 substrate also was varied and 25-, 22-, and 19-residue substrates were tested with the VEEV nsP2 protease (Fig. 2B, Suppl. Fig. S2). As the length of the region N-terminal to the scissile bond decreased, an increase in the K_m was observed consistent with weaker binding.

To determine if the cleavage was specific to the VEEV nsP2 protease, we expressed and purified the proteases of VEEV, EEEV, WEEV and CHIKV. With the 25-residue TRIM14 substrate, complete cleavage of the substrate (50 μM) by the VEEV protease (5 μM) was visible after 24 h at 23 ± 3 °C by SDS-PAGE (Fig. 2C). However, with the shorter TRIM14 substrates the purified CHIKV, EEEV, and WEEV nsP2 proteases only produced low levels of cleavage product even after extensive incubation (64 h, 23 ± 3 °C) (VEEV > WEEV > EEEV > CHIKV) (Suppl. Fig. S2). The corresponding substrates containing the viral cleavage site sequences at the nsP12 junctions also were digested for relative comparison since these proteases differ in activity. The activity of the WEEV and EEEV proteases were the lowest which may be a result of the constructs used. The constructs contain only the nsP2 protease and SAM MTase domains (Fig. 1A and B); these proteases may require an additional domain for full activity (e.g. the ZIKV ns3 protease requires ns2B for full activity (Phoo et al., 2016)). While all four proteases had detectable activity only the VEEV nsP2 cysteine protease consistently cut all of the TRIM14 substrates (Fig. 4E, Suppl. Figs. S2 and S7).

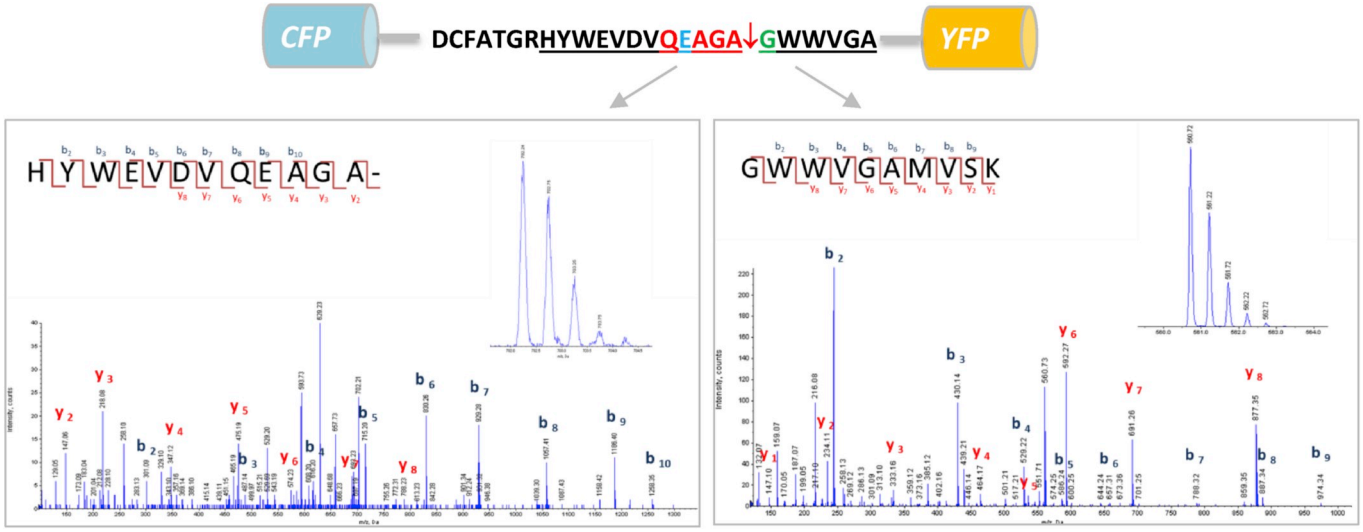

Fig. 3. Mass spectra of the CFP-TRIM14-YFP proteolytic products. Proteolytic products of the CFP-TRIM14–YFP 25-residue substrate after cleavage by the VEEV nsP2 cysteine protease were separated by SDS-PAGE, excised, trypsinized, and identified by tandem mass spectrometry to verify the specificity of the protease. Annotated MS/MS spectra of the HYWEVDVQEAGA and GWWVGAMVSK are shown (enlarged spectra can be found in the Suppl. Info.). For simplicity only singly charged fragments were annotated. All predicted singly charged fragment ions were found.

3.1.2. Modeling of the substrate-bound complexes

To gain insight into the structural basis of substrate specificity, we modeled the binding interactions of TRIM14 with the VEEV nsP2 cysteine protease (Suppl. Fig. S3). Like the New World alphaviral substrates, TRIM14 contains a Glu at position P4 which may explain why no significant cleavage of TRIM14 was observed with the Old World CHIKV nsP2 protease (Figs. 1C and 4E). In the nsP12 cleavage site, the P1′-P6′ residues are identical in sequence for VEEV/EEEV/WEEV, as are the P1-P5 residues. This suggests that residues beyond P5 are important for recognition of the TRIM14 substrate. To understand why the 25-amino acid substrate led to the lowest K_m and highest k_{cat}, we examined our previously determined crystal structure of the free VEEV nsP2 protease, PDB 5EZQ (Hu et al., 2016). The crystal structure contains the C-terminal P2-P19 residues (Leu-776-Ala-792) of the VEEV nsP23 cleavage site; the P10-P19 residues are helical and are packed against the protease domain in the crystal. The P8-P9 residues are directed into the cleft formed by the protease and SAM MTase domains (Suppl. Fig. S4). Chou-Fasman secondary structure predictions suggest that the nsP12 and nsP34 substrates may contain helical regions within the P1-P19 residues.

To understand why the EEEV and WEEV enzymes cut TRIM14 poorly, we examined regions beyond P5 (Suppl. Fig. S3). Based on the K_m values (Fig. 2), the P13-P19 residues of the substrate appear to make additional contacts to the enzyme. In PDB 5EZQ the P17 residue (Ser-778), within the helix of the symmetry related molecule is within hydrogen bonding distance to the backbone NH and C=O of the papain-like protease domain residue Met-555. Met-555 is conserved in the VEEV/EEEV/WEEV nsP2 cysteine proteases. The P19-P16 residues of the substrates differ in charge and flexibility in the New World polyproteins and may be recognized differently by these closely related proteases: “VEEP” in VEEV nsP12; “VDKE” in EEEV nsP12; and “IEKE” in WEEV nsP12. The homologous residues in TRIM14 are “DCFA”. The requirement of an additional domain or motif also cannot be excluded.

To confirm our models of the VEEV nsP2 cysteine protease, we examined cleavage of the TRIM14 substrate by mutants of the protease (Fig. 2C). The K706Q mutation affected the cleavage of V12 and TRIM14 consistent with the disruption of substrate binding interactions in the predicted S4 subsite (Suppl. Fig. S3). The P4 residues (Glu) are the same in both of these substrates (Fig. 1C). The purity of the VEEV nsP2 protease was examined using a C477A variant (Suppl. Fig. S5). Strauss et al. had previously shown that the nonstructural polyprotein was not cut by any intracellular host enzymes in eukaryotic cells (Strauss et al., 1992). Similarly, non-specific cleavage of these protein substrates was not observed with the CFP-YFP substrates expressed and purified from *E. coli*.

3.1.3. Cleavage of the PRY/SPRY domain by the VEEV nsP2 protease

To determine if the cleavage sequence could be cut in the context of the globular PRY/SPRY domain residues 208–442 of TRIM14 were fused to CFP (CFP-PRY/SPRY, 57.7 kDa) and treated with purified VEEV nsP2 protease. Cleavage of the protein in the column fractions containing the PRY/SPRY domain was observed *in vitro* (Figs. 4D and 44.9 kDa product). A shorter truncation product also co-purified and could be cut by the protease. Interestingly, the immunoblots showed poorer detection of the cleaved products when compared with the uncut protein suggesting that the cut protein may more readily aggregate or self-associate, and may enter the gel more poorly.

3.1.4. Confirmation of TRIM14 cleavage in VEEV-infected cell lysates

Sequence alignment analysis shows that full length TRIM14 (442 amino acids, 49.8 kDa) and the TRIM14-α isoform (406 amino acids, 45.1 kDa) contain the cleavage site sequence while the TRIM14–β isoform (28.3 kDa) does not (Suppl. Fig. S6). TRIM14 was shown to be poly-ubiquitinated (Zhou et al., 2014; Jia et al., 2017) and multiple bands were detected in immunoblots (Fig. 4A–C). The anti-TRIM14 antibody used in this work is a Sigma Prestige™ antibody (HPA053217) that has been previously validated and shown to be specific for its antigen in cell lysates and peptide libraries; characterization of this antibody can be found in the Human Protein Atlas (Uhlen et al., 2015). The peptide used to generate this antibody is shown in Suppl. Fig. S6.

The calculated MW of unmodified TRIM14 cleavage products are 37.2 kDa and 12.6 kDa (or 7.9 kDa for the TRIM14α isoform). The recombinant TRIM14 used as a control in the immunoblots is a GST-fusion (~76 kDa). It is important to note that the stability of the cleavage products and the full length protein in cells is unknown, and quantitative conclusions are limited using cell lysates (e.g., calculation of the percentage of TRIM14 cleaved in virus-infected cells). TRIM14 is polyubiquitinated for both degradation (K48-linked) (Jia et al., 2017) and signaling (K63-linked at Lys-365) (Zhou et al., 2014). Overexpression of TRIM14 has been shown to suppress alphaviral replication (Nenasheva et al., 2015) and hepatitis C replication (Wang et al., 2016).

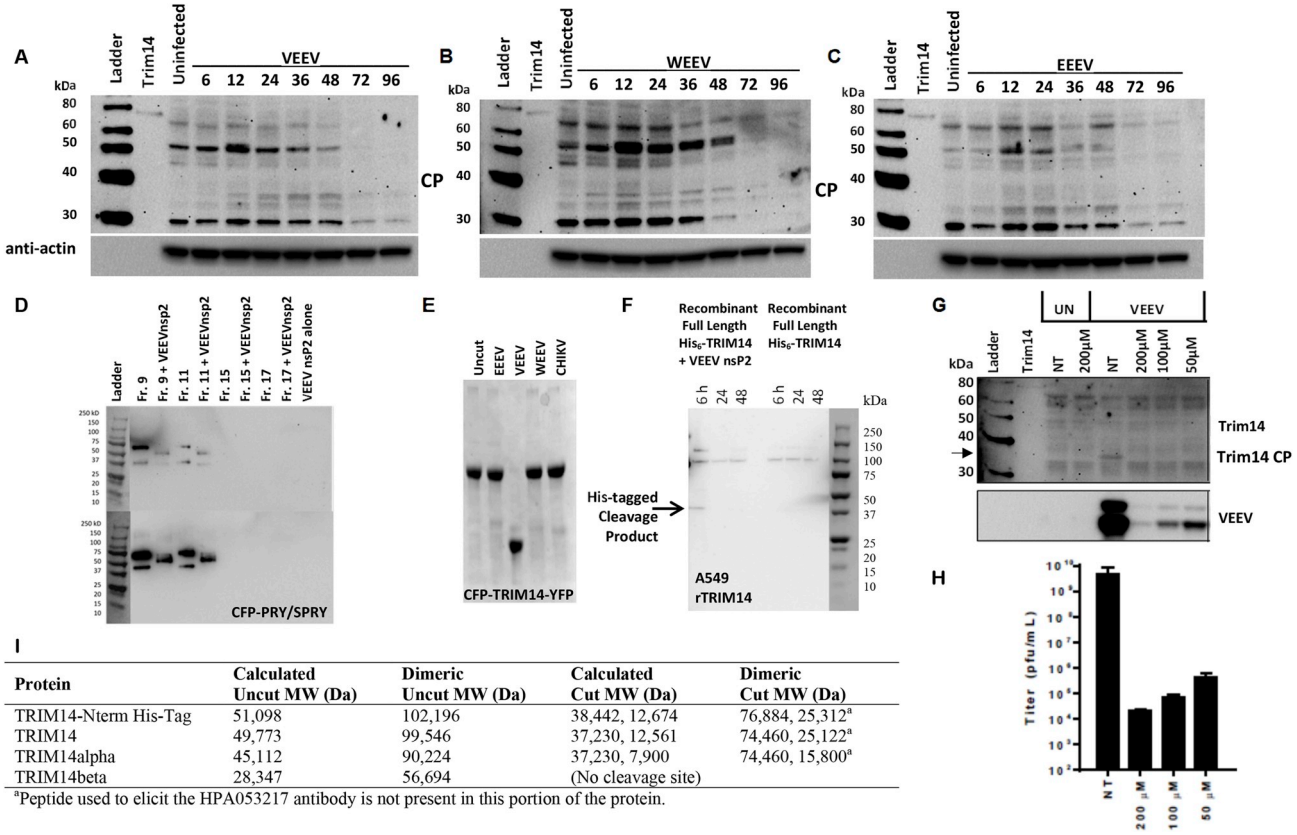

I

Protein	Calculated Uncut MW (Da)	Dimeric Uncut MW (Da)	Calculated Cut MW (Da)	Dimeric Cut MW (Da)
TRIM14-Nterm His-Tag	51,098	102,196	38,442, 12,674	76,884, 25,312[a]
TRIM14	49,773	99,546	37,230, 12,561	74,460, 25,122[a]
TRIM14alpha	45,112	90,224	37,230, 7,900	74,460, 15,800[a]
TRIM14beta	28,347	56,694	(No cleavage site)	

[a]Peptide used to elicit the HPA053217 antibody is not present in this portion of the protein.

Fig. 4. Evidence of VEEV nsP2 protease cleavage of TRIM14 in infected or non-infected cell lysates and *in vitro*. Immunoblots of **(A)** VEEV, **(B)** WEEV, **(C)** EEEV-infected cell lysates using an anti-TRIM14 Prestige polyclonal antibody (HPA053217) that recognizes an epitope common to all 3 isoforms of TRIM14. Cell lysates were removed at various time points (6–96 h). VEEV-infected cell lysates produced a new band with a MW consistent with nsP2 cleavage. WEEV-infected cell lysates also produced a similar band. The cleavage product (CP) band was not detectable in uninfected controls. Multiple bands were observed likely due to the poly-ubiquitination of TRIM14 and the multiple isoforms (α and β) of the protein. **(D)** Cleavage of the CFP-PRY/SPRY domain construct. The upper blot was probed with a mouse anti-Histag antibody (#70796) and reprobed with the Aviva (ARP34737_P050) anti-TRIM14 antibody (lower blot). Aliquots of column fractions were cut with the VEEV nsP2 protease, the uncut control is also shown. A small amount of a truncated protein copurified and also was cut by the protease. **(E)** Purified EEEV, VEEV, WEEV, and CHIKV nsP2 proteases were incubated with the CFP-TRIM14-YFP substrate. Only the VEEV nsP2 protease was able to cleave the TRIM14 protein after 24 h of room temperature incubation. Low levels of CFP-TRIM14-YFP cleavage were observed with purified WEEV nsP2 protease after an extended incubation period (64 h, Suppl. Fig. S2). **(F)** Full length rTRIM14 with an N-terminal His-tag was expressed in A549 cells from pcDNA3.4 plasmids with or without the VEEV nsP2 cysteine protease (tag free). The blot was probed with an anti-Histag antibody and the His-tagged TRIM14 cleavage product was detected after 6 h in the co-transfected cells. The anti-TRIM14 blot is included in the Suppl. Info. **(G)** Inhibition of VEEV nsP2 protease cleavage of TRIM14 by CA074. A549 cells were treated with varying concentrations of a nsP2 cysteine protease inhibitor, CA074 methylester, and then infected with VEEV (multiplicity of infection equal to 10). Cell lysates were examined by immunoblot analysis using the anti-TRIM14 antibody HPA053217. The TRIM14 CP was present in the infected cells that had not been treated with the protease inhibitor (labeled NT for "not treated") and was absent in cell lysates treated with the nsP2 cysteine protease inhibitor. Infection was confirmed by immunoblot analysis using anti-VEEV sera in the lower blot. **(H)** Plaque assay of cell lysates in (G) showing a reduction in PFU/mL in the presence of increasing concentrations of CA074me, an inhibitor of the VEEV nsP2 protease. **(I)** Calculated MW of each isoform and cleavage product.

TRIM14 cleavage in VEEV-infected cells was monitored over time and cell lysates were collected at 6, 12, 24, 36, 48, 72, and 96 h. The band intensities varied over time; however, only the VEEV- and WEEV-infected cell lysates contained a new ~37 kDa cleavage product that was not found in the uninfected controls (Fig. 4A and B). The 50 kDa band intensified during infection and may be due to enhanced expression of TRIM14 during viral infection. TRIM14 expression can be detected in the absence of virus (Zhou et al., 2014) indicating that this protein is an intrinsic immune response effector protein. TRIM14 expression also can be further induced by IFN and also can be considered an innate immune response effector (Carthagena et al., 2009). The MW of the cleavage product was consistent with the calculated MW and with the *in vitro* results using purified recombinant nsP2 proteases, the CFP-PRY/SPRY domain construct (Fig. 4D), and the 25-, 22-, and 19-residue CFP-YFP TRIM14 substrates (Fig. 2, Suppl. Fig. S2). A549 cells (human lung carcinoma, Sigma-Aldrich 86012804, HPA Culture Collection) also were co-transfected with a plasmid expressing full length His-tagged TRIM14 and a tag-free VEEV nsP2 cysteine protease (sequence is shown in the Suppl. Information). Cells were collected at 6, 24, 48 h. In the virus-infected cells, the cleavage product was observed at the 24 h time point (Fig. 4A). In the co-transfection experiment (CMV promoter) the cleavage product could be detected transiently at the 6 h point and was short lived (Fig. 4F, Suppl. Fig. S7). At the 24 h point a transient decrease in the TRIM14 band intensities also was observed (Suppl. Fig. S7). The early appearance of degradation product also was reported for feline calicivirus (FCV) (observed between 5 and 8 h) (Kuyumcu-Martinez et al., 2004a) and for foot-and-mouth disease virus (FMDV) (within 2 h) (Grigera and Tisminetzky, 1984). Thus, these proteolytic cleavages may occur early in virus-infected cells (≤24 h).

TRIM14 may be cleaved before or after poly-ubiquitination; since the cleavage site precedes Lys-365, cleavage of the two species cannot be distinguished. Upon viral infection Lys-63-linked polyubiquitination of TRIM14 at Lys-365 occurs and was shown to be important for the assembly of the MAVS signalosome (Zhou et al., 2014) (Figs. 5 and 6). Thus, cleavage of TRIM14 may interfere with the assembly of the MAVS signalosome.

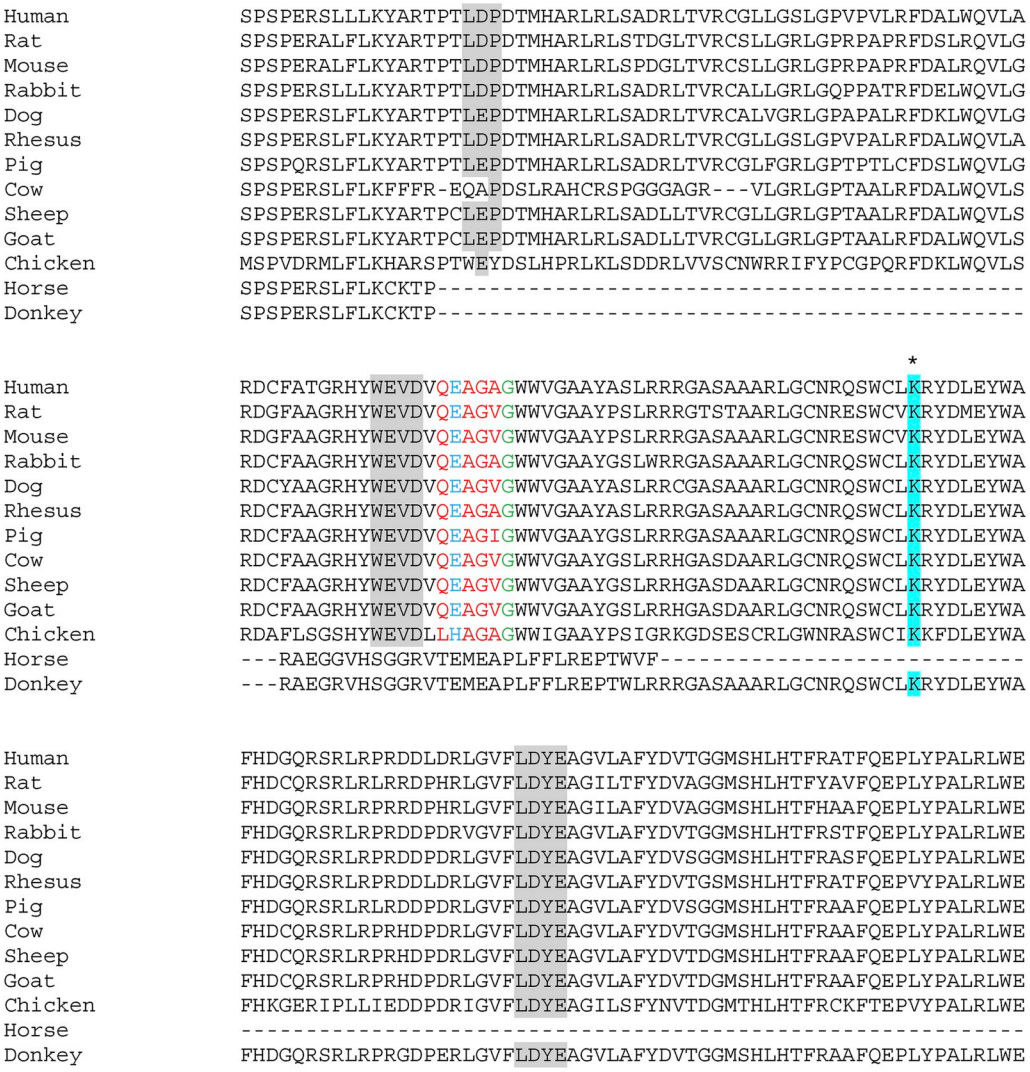

Fig. 5. Partial sequence alignment of the C-terminal domain of TRIM14 homologues from other species. The region shown contains the predicted PRY/SPRY domain of the TRIM14 protein. In gray are the PRY/SPRY domain motifs ("LDP", "WEVD", "LDYE"). The QEAGA↓G motif is shown in red, blue, and green. In human TRIM14 Lys-365 (highlighted in cyan and labeled with an asterisk) was shown to be poly-ubiquitinated. This ubiquitination site is important for recruitment of NEMO to the MAVS signalosome (Zhou et al., 2014).

3.1.5. TRIM14 cleavage in VEEV-infected cells can be inhibited by the nsP2 cysteine protease inhibitor CA074me

CA074 methyl ester (CA074me) previously was shown to inhibit the alphaviral VEEV nsP2 cysteine protease (Campos-Gomez et al., 2016). CA074me is a Cathepsin B inhibitor; however, no other host enzymes have been shown to cleave the nonstructural polyprotein (Strauss et al., 1992). CA074 is a peptide-like irreversible covalent inhibitor that specifically reacts with the nucleophilic Cys of the proteases. CA074me is the membrane permeable form of the CA074 inhibitor (prodrug). CA074me was added to cells that were infected with VEEV; cell lysates were collected and subjected to immunoblotting. The TRIM14 cleavage product was no longer present in the CA074me-treated cells, consistent with inhibition of the VEEV nsP2 cysteine protease (Fig. 4G). Higher viral titers (plaque forming units (PFU) per mL) in plaque assays were observed when the cleavage product was present and detectable (Fig. 4H). In the presence of the CA074me, lower titers (~4-log lower) are observed and the TRIM14 cleavage product is no longer detectable (Fig. 4H).

3.2. Prediction of four ZIKV ns2B/ns3 host protein substrates and their roles in vivo

The ZIKV ns2B/ns3 protease cleavage site sequences in the nonstructural polyprotein of ZIKV have been published and are shown in Fig. 7A (Shiryaev et al., 2017). Each site was inputted into BLAST; the highest sequence identity matches were obtained with the cleavage site sequence at the ns3/ns4A junction followed by the cleavage site sequences at the ns2A/ns2b and ns2B/ns3 junctions (Suppl. Fig. S8). Human SFRP1 had a stretch of 11 residues that matched the subsite tolerances of the ZIKV ns2B/ns3 protease, nine of which were consecutive in order. The next three proteins with high sequence similarity to the viral cleavage sites were: a retinal G_s alpha subunit; a mitochondrial deoxyribonucleotidase (NT5M); and the Forkhead box protein G1 (FOXG1). CFP-YFP substrates were made for each of these host proteins (sequences can be found in the Suppl. Info.). To confirm the specificity of the protease and the accuracy of the prediction, we also included CFP-YFP substrates for SFRP2 and SFRP4 since these isoforms had sequences similar to SFRP1 (Fig. 7C). Two of the predicted cleavage sites were present within the signal peptide or predicted signal peptide sequence. This may be significant since flaviviral proteases are anchored to the endoplasmic reticulum (ER) membrane (Romero-Brey and Bartenschlager, 2016); it also suggests that co-translational cleavage events cannot be ruled out. The ZIKV protease domain is thought to be on the cytoplasmic face of the ER, whereas the signal peptidase is in the interior of the ER lumen.

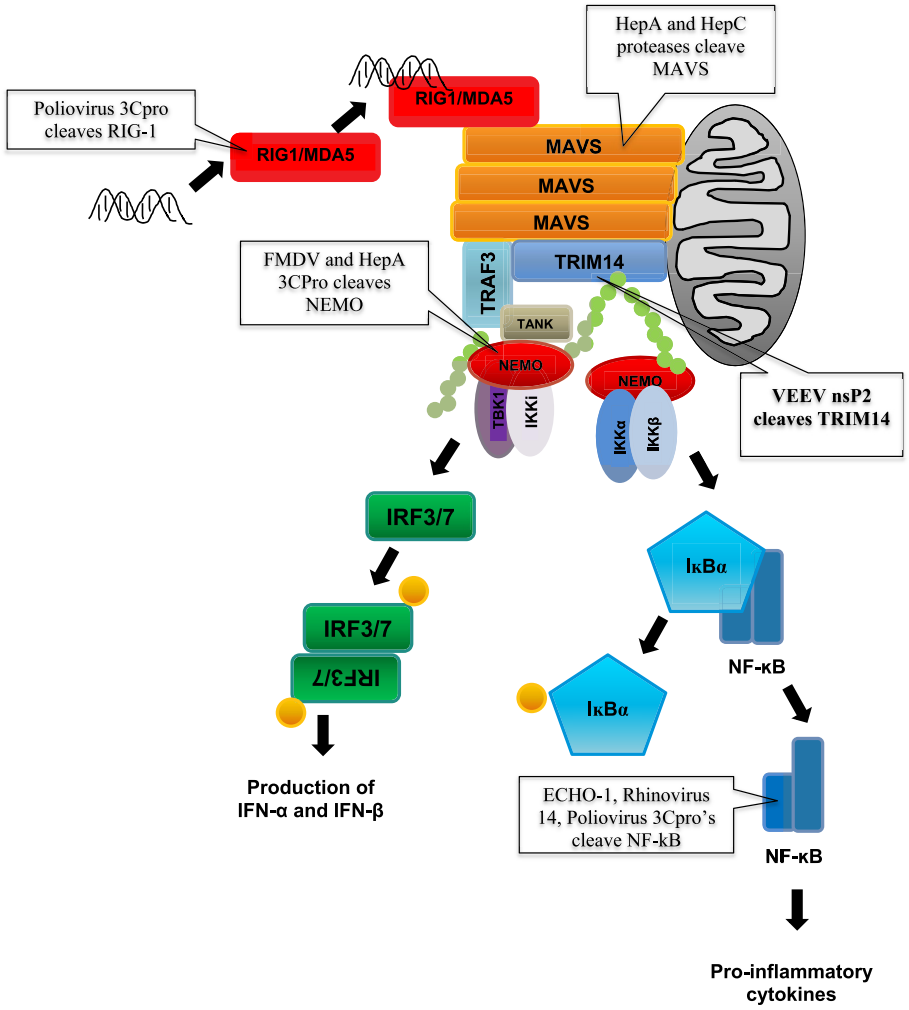

Fig. 6. Several Group IV (+)ssRNA viral proteases cleave components of the MAVS signalosome. The MAVS signaling cascade proposed by Zhou et al. is shown (Zhou et al., 2014). The MAVS signalosome triggers the production of IFN and pro-inflammatory cytokines. The VEEV nsp2 cysteine protease cleavage site in TRIM14 is located before the ubiquitination site. Cleavage of the proteins involved in the signalosome likely would disrupt the production of IFN and the innate immune response (Neznanov et al., 2005; Barral et al., 2009; Yang et al., 2007; Meylan et al., 2005; Wang et al., 2012).

Several of the predicted substrates were involved in early development, bone remodeling, neuronal or brain development. Two of the predicted substrates were associated with Smith-Magenis syndrome (NT5M, MID51) and FOXG1 was associated with FOXG1 syndrome; both are syndromes that have been associated with microcephaly (Kortum et al., 2011; Gropman et al., 2006). SFRP1 has been associated with Mowat-Wilson syndrome (Miquelajauregui et al., 2007), another syndrome associated with microcephaly.

3.3. *In vitro evidence of ZIKV ns2B/ns3 host protein cleavage*

3.3.1. *ZIKV ns2B/ns3 cleaves SFRP1, but not SFRP2 or SFRP4*

The top predicted substrate of the ZIKV ns2B/ns3 protease, SFRP1, plays a role in developmental patterning, but also in innate immunity. Wnt proteins (16 different ones) are secreted glycoproteins that bind and activate intracellular signaling cascades when bound to their receptor, Frizzled. Secreted frizzled-related proteins (SFRP) are soluble receptors that also can bind Wnt ligands (competitively) to antagonize and inhibit Wnt signaling. The Wnt pathway also is linked to IFN-γ production; the addition of SFRP1 suppresses the production of IL-4 and increases the production of IFN-γ by T-cells (Lee et al., 2012). Thus, proteolytic cleavage of SFRP1 could antagonize the production of IFN-γ to suppress its antiviral effects. The Wnt signaling pathway was previously linked to the regulation of the IFN response during Flavivirus infection; microRNAs that repressed Wnt/β-catenin signaling had strong anti-flaviviral effects (Smith et al., 2017). Thus, the proteolytic cleavage of SFRP1 would be expected to enhance flavivirus replication.

Bodine et al. characterized SFRP1 (−/−) knockout mice and reported decreased brain weights, increased heart weights, and abnormal trabecular bone morphology (Bodine et al., 2004); however, SFRP1 was not found to be essential for normal embryonic development. SFRP1 is expressed in the neural tube caudal to the hindbrain; the mRNA is expressed in the proliferative zone of developing neurons (Bodine et al., 2004; Augustine et al., 2001). Early in development SFRP1 expression is found in the brain, eye, ear, lower abdomen, and upper spine (Trevant et al., 2008); it also is found in regions of the skeleton undergoing new bone formation (at growth plates). After birth, strong expression continues in the brain, heart, and kidneys. Abnormalities in the kidneys of SFRP1 (−/−) mice are not observed at 1 year of age (Trevant et al., 2008). SFRP1 and SFRP5 are close homologues (51% identity); however, SFRP5 does not contain an "RG" sequence in its N-terminus. Both are expressed in the retina and may be involved in determining the polarity of photoreceptor cells in the retina (Chang et al., 1999; Marcos et al., 2015; Esteve et al., 2011). When SFRP1 and SFRP2 are both absent, a craniofacial abnormality is observed (Satoh et al., 2006). Alignment of the N-terminal sequences of SFRP1, SFRP2, and SFRP4 show that each have a "RG" sequence, and ≥4 residues are similar to a viral polyprotein cleavage site (Fig. 7C). Substrates

A

Substrate	Cleavage Site Sequence	Accession No.
ZIKV C↓Ci	KER**KRR**↓**GADT**SIGI	
ZIKV ns2A↓ ns2b	TRS**GKR**↓**SWPP**SEVL	
ZIKV ns2B↓ns3	VKT**GKR**↓**SGAL**WDVP	
ZIKV ns3↓ns4A	FAA**GKR**↓**GAAL**GVME	
ZIKV ns4B↓ns5	GLV**KRR**↓**GGGT**GETL	
Secreted Frizzled-related protein 1 (SFRP1)	SEGGRR↓GAALGVLL	NP_003003.3, AAB70793.1
Gs Alpha subunit	QVAGRR|GAALPCSL	CAA39484.1
NT5M, 5'(3')-deoxy-ribonucleotidase, mitochondrial isoform X3	VPAGRR|GAAGGLGL	XP_011522268.1
Transcription factor HFK1 (Forkhead box protein G1)	KLAFKR|GARLTSTG	CAA52239.1
Ankyrin repeat domain-containing protein 65 isoform 1	AAAAGR|GAALRFLL	NP_001138682.1
Mitochondrial dynamics protein MID51 isoform 1	SHSGKR|SWEEPNWM	NP_061881.2
Voltage-dependent T-type calcium channel subunit alpha-1H isoform X7	GPPARR|SWPPSPQR	XP_016879309.1
Plexin-B3 isoform 1 and 2 precursor & plexin-B3	FAAGPR|GTQAALCA	NP_005384.2
PRRC2A	GRGDKR|SWPSPKNR	AQY77357.1
Leucine-rich repeat and calponin homology domain-containing protein 4 isoform 2	TEAGQR|GSALGDLA	NP_001276863.1
Protein phosphatase 1B (PPM1B)	RAAGKS|GSALELSV	AAY89640.1
FCRLB protein	GPREAR|GAALGGVV	AAH38564.2

B

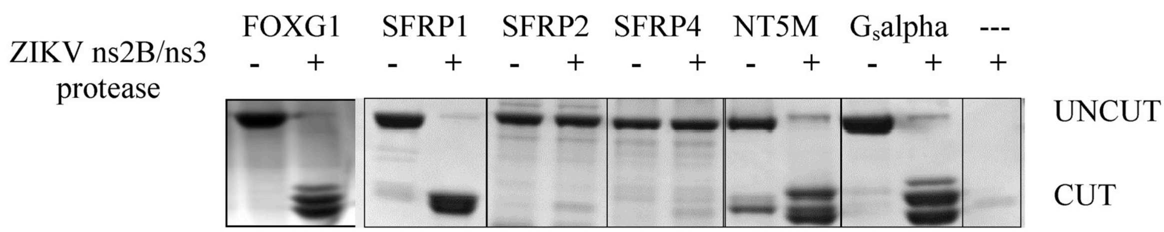

C

```
SFRP1                  MGIGRSEGGRRGAALGVLLALGAAL
SFRP2       MLQGPGSLLLLFLASHCCLGSARGLFLFGQPDFS
SFRP4          MFLSILVALCLWLHLALGVRGAPCEAVRIPMCRH
```

D

```
                               SFRP1                       FOXG1               NT5M
                                 ↓
ZIKV ns2B|ns3             VKTGKRSGALWDVP
ZIKV ns3|ns4A             FAAGKRGAALGVME                         ↓                    ↓
Homo sapiens          MGIGRSEGGRRGAALGVLLALGAAL   RSTTSRAKLAFKRGARLTSTG   CSAAVPAGRRGAAGGLGLAGG
Macaca mulatta        MGSGRSAGGCRGAALGVLLALGAAL   RSTTSRAKLAFKRGARLTSTG   CSAAVPAGRRGAAGGQGLAGG
Gorilla gorilla       MGSGRSVGGRRGAVLGVLLALGAAL   RSTTSRAKLAFKRGARLTSTG   CSAAVPAGRRGAAGGPGLAGG
Pongo abelii          MGSGRSVGGRRGAALGVLLALGAAL   RSTTSRAKLAFKRGARLTSTG   CSAAVPVGRRGAAGGPGLAGD
Pan troglodytes       MGSGRSVGGRRGAALGVLLALGAAL   RSTTSRAKLAFKRGARLTSTG   CSAAVPAGRRGAAGGPGLAGG
Myotis lucifugus      MGSGRGAGGRRGAAGGVLLALAAGL    (seq unavailable)      ---------------------
Tupaia chinensis      MGSGRGAGGRRGAAAGVLLALAAGL   RSTTSRAKLAFKRGARLTSTG   ---------------------
Gallus gallus         MGVGRSEGGRRGAALGVLLALGVAL   RSTTSRAKLAFKRGARLTSTG   HCGPLAGLGRGSCPTAGSRRA
Equus caballus        MGSGRGAGGRRGAAGGVLLALAAGL   RSTTSRAKLAFKRGARLTSTG   RGAAGPAGRRWAAGGPAGRAG
Xenopus laevis        -----MNGENGIWPLLLFWVTPGIL   RSTTSRAKLAFKRGARLTSTG   MAFLPSLLRRGNMLSPRLQNS
Bos taurus            ------MGGGRWAAAGALLALAAGL   RSTTSRAKLAFKRGARLTSTG   RGAAGPAGRRWASGGPAGRA-
Sus scrofa            ------MGGGRWAAAGVLLALAAGL   RSTTSRAKLAFKRGARLTSTG   TRPAGPAGRRWASGGPGGRA-
Camelus dromedarius   ------MGGGRWAAAGVLLALAAGL   RSTTSRAKLAFKRGARLTSTG   -MAMAMAARHTRP--------
Rattus norvegicus     MGVGRNARGRGGAASGVLLALAAAL   RSTTSRAKLAFKRGARLTSTG   RLRGCCARPRGAPLRAER---
Mus musculus          MGVGRSARGRGGAASGVLLALAAAL   RSTTSRAKLAFKRGARLTSTG   RLRGCCARPRGAPLRAERSR-
Salmo salar           ----MRSIERLCGWRIIPLALTMAV   RSTTSRAKLAFKRGARLTSTG   GRILLHDQFKCISAKMSSSSG
C. elegans            ----------MMLFPVLYILFAFSV   RPSS------------LSRAR       (No homologue)
```

Fig. 7. Cleavage of four host protein sequences by the ZIKV ns2B/ns3 protease. **(A)** The viral polyprotein cleavage site sequences and top 12 hits from BLAST searches. **(B)** SDS-PAGE gel of CFP-YFP substrates containing human host protein sequences. The top 4 predicted substrates were cut by the ZIKV ns2B/ns3 protease. The ZIKV protease alone is shown in the last lane; the + and – symbols indicate which reactions contained the enzyme. CFP-YFP substrates containing two related protein sequences from SFRP2 and SFRP4 were included as controls. These proteins were not predicted to be substrates of the ns2B/ns3 protease and no cleavage was observed. Reactions were run for 19 h at room temperature using 20 μM substrate and 2 μM enzyme. Reactions not containing enzyme were run alongside ("-") and incubated for the same period. A truncation product co-purified with the NT5M substrate which contained cysteines; however, the cleavage products still were readily discernible. **(C)** Sequence similarity in the signal peptides of SFRP1, SFRP2, and SFRP4. Each contain the "RG" sequence. **(D)** Alignment of SFRP1, FOXG1, and NT5M cleavage site sequences from various animal species. In red are residues that are identical to a viral cleavage site motif sequence. In green are residues that are tolerated at the subsite in other viral polyprotein cleavage sites. The arrow denotes the scissile bond.

containing the human SFRP1, SFRP2, and SFRP4 signal peptide sequences were tested (Fig. 7B); however, only the predicted SFRP-1 signal peptide sequence could be cleaved by the ZIKV ns2B/ns3 protease *in vitro*, consistent with the high sequence specificity requirements of a viral protease.

Alignment of SFRP1 from multiple animal species (Fig. 7D) shows that the cleavage site sequence differs in SFRP1 homologues from rodents, whereas high sequence similarity is found in the SFRP1 homologue of chickens. Notably, Goodfellow et al. recently showed that ZIKV can induce mortality and microcephaly in chicken embryos (Goodfellow et al., 2016). ZIKV has been shown to efficiently infect fibroblasts of New and Old World monkeys, but not rodents (Ding et al., 2018). Only immunocompromised mice have been infected with ZIKV and have produced signs of microcephaly (Cugola et al., 2016). The alignment of the cleavage site sequence of SFRP1 is consistent with these observations. SFRP1 from brown bats (*Myotis lucifugus*) also had sequence similarity with the cleavage site sequence; infection of these bats with ZIKV produces neurological symptoms (Kading and Schountz, 2016; Reagan et al., 1955).

3.3.2. ZIKV ns2B/ns3 cleaves an alpha subunit of a G-protein

This G_s alpha subunit (CAA39484.1) was previously isolated from human adult retina and fetal eye cDNA libraries (EMBL database accession number X56009) (Swaroop et al., 1991). This G_s alpha subunit shares sequence identity (~80%) with a G_s alpha subunit in a G-protein coupled calcitonin receptor and a cryo-EM structure of the G-protein coupled receptor is known (PDB 5UZ7) (Liang et al., 2017). The ZIKV ns2B/ns3 protease cleaved the G_s alpha subunit sequence (Fig. 7B). While the C-terminal region of this protein aligned well with homologues from other species, the N-terminal region containing the cleavage site did not.

3.3.3. ZIKV ns2B/ns3 cleaves NT5M mitochondrial 5′,3′-nucleotidase

This enzyme also is known as dNT-2 (XP_011522268.1, Q9NPB1) and is encoded within the Smith-Magenis syndrome region of chromosome 17. NT5M is localized to the mitochondrial matrix, and its N-terminus contains a predicted mitochondrial targeting sequence. The predicted cleavage site of the mitochondrial processing peptidase (MPP) is C-terminal to the predicted ZIKV ns2B/ns3 cleavage site. NT5M is thought to regulate levels of pyrimidine deoxyribonucleotides in the mitochondria, but its role in disease is unclear (Rampazzo et al., 2000). The ZIKV ns2B/ns3 protease cleaved the NT5M sequence (Fig. 7B). Sequence alignments with homologues from other species showed high sequence identity to this cleavage site among primates and sporadic sequence identities with other species (Fig. 7D).

3.3.4. ZIKV ns2B/ns3 cleaves Forkhead box protein G1

Forkhead box protein G1 (FOXG1) is a transcription factor encoded by the *FOXG1* gene. FOXG1 is involved in brain development, specifically in the telencephalon. Mutations of this gene lead to FOXG1 syndrome. FOXG1 syndrome initially was considered to be a variant of Rett syndrome (a syndrome which only affects females) (Pratt et al., 2013), but was reclassified as an autism spectrum disorder since FOXG1 syndrome affects both males and females (Mariani et al., 2015). It is characterized by microcephaly (congenital or postnatal) (Kortum et al., 2011; Jacob et al., 2009) and brain malformations (Ma et al., 2016). FOXG1 is also linked to the Wnt/β-catenin signaling pathway in the retina (Fotaki et al., 2013). In adults FOXG1 plays a role in neuronal survival (Dastidar et al., 2012). The ZIKV ns2B/ns3 protease cleaved the FOXG1 sequence embedded in between CFP and YFP (Fig. 7B). The cleavage site sequence was highly conserved across species (Fig. 7D).

4. Discussion

4.1. Comparison of TRIM14 homologues from different species

For acute viral infections, the host possesses antiviral enzymes and proteins that interfere with and counter viral replication (sometimes referred to as viral restriction factors). One domain within TRIM14 appears to be important to its antiviral functions and may account for species-specific anti-alphaviral responses (Wang et al., 2016). Human VEEV infections rarely result in lethal encephalitis (~1% of infected humans), whereas the mortality rate in equine is significantly higher (e.g., EEEV's mortality rate can be as high as 90% in horses) suggesting an inherent difference in the innate immune response pathways of equid vs. humans. Comparison of TRIM14 homologues from various species shows strong conservation of the full length TRIM14 sequence in humans, monkeys, rodents, pigs, cows, and chickens (Fig. 5). In contradistinction, the C-terminal region of equid TRIM14 is notably truncated. The C-terminal region of TRIM14 was predicted to form a PRY/SPRY domain. The VEEV nsP2 cysteine protease cleavage site is within this predicted domain. The SPRY domain is a β-stranded protein interaction module commonly found in human proteins that regulate innate and adaptive immunity (D'Cruz et al., 2013). The PRY motif consists of three additional β-strands N-terminal to the SPRY domain. PRY/SPRY domains can be identified by three highly conserved sequence motifs (“LDP”, “WEVD/E”, “LDYE/D”). These three motifs are present in the human TRIM14 homologue but are absent from the equine TRIM14 homologue (Fig. 5). Interestingly, the donkey homologue contains the “LDYE” motif, but lacks the other two motifs. PRY/SPRY domains contain hypervariable loop regions and a conserved core similar to a variable domain of an antibody (James et al., 2007). The binding specificity of the SPRY domain determines the function of the TRIM protein and mutations within this domain have been associated with disease susceptibility (James et al., 2007). This domain appears to be important for mounting an effective immune response against alphaviruses, as well as hepatitis C virus (HCV) (Wang et al., 2016). The transient proteolytic cleavage of the PRY/SPRY domain during infection, or the absence of this domain as in the case of equine TRIM14, may impair a species' ability to mount an effective antiviral immune response to alphaviruses.

The presence or absence of the PRY/SPRY domain of TRIM14 was not sufficient to predict the virulence or pathogenicity of VEEV in other species, e.g., VEEV infections can be lethal in mice, and the murine TRIM14 contains the PRY/SPRY domain. The role of TRIM14 and the downstream effectors (i.e. IFN-stimulated genes, ISG) of this pathway have not been examined across species and may differ. Species-specific differences in the Jak/STAT pathway, a pathway triggered by type I IFN, also cannot be excluded.

TRIM14 has been proposed to function as an adaptor molecule in the MAVS signalosome (Zhou et al., 2014) (Fig. 6). The PRY/SPRY domain is thought to mediate the association of TRIM14 to the C-terminal domain (residues 360–540) of MAVS (Zhou et al., 2014). TRIM14 undergoes ubiquitination at a site within the PRY/SPRY domain at Lys-365 and recruits NF-κB essential modulator (NEMO) to activate the IFN regulatory factors 3 and 7 (IRF-3/7) and NF-κB pathways (Zhou et al., 2014). The ubiquitination of Lys-365 was shown to be critical for the association of NEMO to the MAVS signalosome by Zhou et al. (2014). Phosphorylation of IRF-3 leads to the production of type I IFNs. The VEEV nsP2 cysteine protease cleavage site is 31 residues before Lys-365 and cleavage likely short circuits this cascade to prevent its downstream effects.

4.1.1. Significance of TRIM14 cleavage

TRIM proteins exert a variety of interfering effects in response to intracellular pathogens, predominantly against retroviruses (Nisole et al., 2005), but also have been shown to have antiviral activities against other types of viruses (Carthagena et al., 2009; Munir, 2010;

Ozato et al., 2008). TRIM proteins typically contain three domains: (1) a RING finger domain; (2) B-box zinc finger domain(s); and a (3) coiled-coil domain. In addition to these three domains, TRIM proteins have variable C-terminal domains often which contain SPRY or PRY/SPRY domains that define the specific function of the TRIM protein (James et al., 2007).

TRIM proteins can function as intrinsic or innate antiviral factors (Carthagena et al., 2009). Intrinsic immune factors are proteins that are present prior to viral infection, while innate immune factors are those that are generated after viral infection (Bieniasz, 2004; Yan and Chen, 2012). Expression of slightly less than half of all known TRIM proteins is induced by type I or type II IFN, or both (Carthagena et al., 2009). Other TRIM proteins are constitutively expressed (Carthagena et al., 2009). TRIM proteins can act as viral restriction factors (e.g. TRIM5α and HIV (Malim and Bieniasz, 2012)). Several TRIM proteins are ubiquitin E3 ligases. However, a subset of TRIM proteins lack a RING domain (e.g. TRIM14, TRIM16, TRIM16L, TRIM20, TRIM29, TRIM44, TRIM51, TRIM66) and are not thought to harbor the activity (Zhou et al., 2014; Carthagena et al., 2009). The function of TRIM14 is thought to be more general; TRIM14 localizes to the outer membrane of mitochondria and has been proposed to function as an adaptor in the mitochondrial antiviral-signaling protein (MAVS, also known as IPS-1/VISA/Cardif) signalosome (Zhou et al., 2014). The MAVS cascade leads to the production of IFN and proinflammatory cytokines (Bhoj et al., 2008).

Stable overexpression of TRIM14 has been shown to inhibit alphaviral replication (SINV) by 3–4 logs 24 h post-infection (Nenasheva et al., 2015) consistent with TRIM14's proposed role in the innate immune response (Zhou et al., 2014). TRIM14 overexpression also increases the transcription of IFNs and ISGs (Nenasheva et al., 2015) consistent with the pathway proposed by Zhou et al. (2014) (Fig. 6). Other lines of evidence support the conclusion that TRIM14 is an adaptor protein involved in the MAVS signalosome such as co-localization of TRIM14 and RIG-1 and MAVS (Tan et al., 2017). However, other antiviral mechanisms involving TRIM14 also are possible. For example, the HCV ns3/4A protease cleaves MAVS and TRIF, components of two different interferon generating pathways (Table 1). Wang et al. demonstrated that TRIM14 overexpression inhibited infection by and replication of HCV while TRIM14 knockout cells became more susceptible to HCV infection (Wang et al., 2016). Using a K365R variant of TRIM14 (labeled in Fig. 5) they found that the antiviral activity of the TRIM14 variant was comparable to that of the wild type TRIM14. Since Lys-63-linked polyubiquitination of K365 of the PRY/SPRY domain is important for MAVS signalosome assembly (Zhou et al., 2014), this suggests that TRIM14 may have another role in a different antiviral mechanism.

4.2. General significance of host protein cleavage by viral proteases

The proteolytic cleavage of components of the MAVS signalosome and the toll-like receptor pathways by viral proteases appears to be a common mechanism for innate immune response evasion by Group IV (+)ssRNA viruses. While several examples of this phenomena were known (Table 1) and several had been predicted (Kiemer et al., 2004), they had not been previously compared. There are now ~30 cases of host protein-viral protease cleavages (Table 1). From the table, it is apparent that the viral proteases which predominantly utilize this strategy belong to Group IV. However, a Group VI (+)ssRNA retroviral protease (HIV protease) also has been shown to cleave poly(A)-binding protein (PABP) (Alvarez et al., 2006). Second, the host protein targets were generally involved in generating innate immune responses suggesting that these short sequences are being used for targeted destruction of host innate immune response proteins. Some had obvious roles (e.g. proteins belonging to the MAVS signalosome and proteins like TRIF that belong to toll-like receptor pathways that lead to the production of IFN-β), whereas others had more obscure relationships (e.g. histone H3). The cleavage of histone H3 by the FMDV 3C protease was one of the earliest reported in 1984 (Grigera and Tisminetzky, 1984; Falk et al., 1990). The first 20 amino acids of histone H3 are cleaved by the FMDV 3C protease. It was later shown that H3 is hyperacetylated at the IFN-β promoter during viral infection (Parekh and Maniatis, 1999; Qiao et al., 2016) and acetylation at Lys-14 is common in genes that are being actively transcribed.

Cleavage of several of the targets in Table 1 also could facilitate the shutoff of host transcription and translation. For example the 3Cpro of viruses belonging to *Picornaviridae* have been shown to cleave RNA polymerase II transcription factors, TATA-binding protein (Clark et al., 1993; Kundu et al., 2005), CREB (cAMP responsive element binding protein), Oct-1, p53, RNA polymerase III transcription factor IIIC (Clark et al., 1991), Polymerase I factor SL-1 (Weidman et al., 2003), PABP (Kuyumcu-Martinez et al., 2002, 2004a), eIF5B (de Breyne et al., 2008), eIF4AI (Li et al., 2001), and eIF4GI (Foeger et al., 2002). The *Picornaviridae* proteases have also been shown to cleave TRIF (Qu et al., 2011), RIG-I (Barral et al., 2009), MDA-5 (Barral et al., 2007), MAVS (Yang et al., 2007), NF-κB (Neznanov et al., 2005), DNA-PK (Graham et al., 2004), and NEMO (Wang et al., 2012, 2014). Calicivirus 3C-like protease (*Caliciviridae*) also cleaves PABP (Kuyumcu-Martinez et al., 2004a). The HCV viral ns3/4A protease (*Flaviviridae*) was shown to cleave MAVS (Lin et al., 2006; Hiscott et al., 2006; Bellecave et al., 2010; Meylan et al., 2005). TRIF (TIR-domain-containing adapter inducing interferon-β) was a common target of viral proteases (Qu et al., 2011; Li et al., 2005a). The Dengue and Zika viral ns2B/ns3 proteases were shown to cleave STING (stimulator of the interferon gene, also known as a MITA, mediator of IRF3 activation) (Ding et al., 2018; Yu et al., 2012), a protein that can interact with RIG-I and MAVS, but not with MDA-5. Cleavage of STING by the Dengue viral protease led to the inhibition of type I IFN production (Yu et al., 2012; Aguirre et al., 2012; Li et al., 2005b). Here we have shown that the VEEV nsP2 protease (*Togaviridae*) can cleave TRIM14 and that the ZIKV ns2B/ns3 protease (*Flaviviridae*) can cleave sequences within SFRP1, a retinal G_s alpha subunit, the NT5M deoxyribonucleotidase, and FOXG1. These biochemical results may warrant further investigation by other methods.

The characteristic cleavage products of viral proteases may produce valuable biomarkers of viral infection and could be useful in the selection of therapeutics (i.e. antiviral protease inhibitors) that can interfere with the virus-induced phenotype. MAVS cleavage products were observed in humans with chronic HCV infections but not in controls and the cleavage of MAVS by the HCV ns3/4A protease was associated with higher viral loads (Bellecave et al., 2010). Since biomarkers for alphaviral infections are relatively uncharacterized, the cleavage of TRIM14 or the downstream effects of cleavage, or both, may be useful indicators of VEEV infection. The cleavage of TRIM14 by the VEEV nsP2 cysteine protease may also have therapeutic value since TRIM14 overexpression has also been associated with cancer (Hu et al., 2018; Su et al., 2016; Xu et al., 2017).

Knowledge of the host protein substrates of Group IV viral proteases may also provide another parameter for assessing the ability of an animal model to reproduce the virus-induced phenotype. Animal models that faithfully recapitulate the virus-induced phenotype are important for therapeutics discovery and for the evaluation of vaccines. From sequence alignments the viral protease cleavage site motif sequence in the SFRP1 homologue of chickens had very high sequence identity with the human homologue (i.e. the EGGRRGAALGV sequence is identical in both species). The cleavage site sequences in FOXG1 were also identical. ZIKV infection of chicken embryos produces microcephaly (Goodfellow et al., 2016). Thus, the host protein cleavage site sequences may be useful for the selection of an animal model or a cell line. The SFRP1 sequences of rodents did not align well in this region, consistent with other observations regarding ZIKV host tropism (Ding et al., 2018). Interestingly, decreases in mRNA levels of FOXG1 and a Wnt signaling protein called LHX2 were reported in neural progenitor cells of Zika affected twins compared with non-affected twins (Caires-

Table 1
Group IV viral proteases that have been shown to cleave host-proteins involved in the innate immune response. In bold are the proteins involved in IFN production pathways. In bold-italics are the residues that are identical to a single viral polyprotein cleavage site, in italics are residues which are found at the same position in other viral polyprotein cleavage sites.

Virus	Family	Viral Protease	Viral Protease Cleavage Site Motif	Host Protein Substrate	Cleavage site in Host protein	Reference
Poliovirus	*Picornaviridae*	3Cpro	(QE)↓(LIGS)	**RIG-1**	LKKFP***Q***↓***G***QKGKV	Barral et al. (2009)
				TATA-binding Protein	QGL*A*SP***Q***↓***GA***M*T*PG	Das and Dasgupta (1993)
				TATA-binding Protein	AA*A*VQ***Q***↓STSQQA	Kundu et al. (2005)
				Poly(A)-binding protein (PABP)	*V*H***VQ***↓***G***Q	Kuyumcu-Martinez et al. (2004b)
				eIF5B	***VMEQ***↓***G***	de Breyne et al. (2008)
		2Apro		TATA-binding Protein	MMP***Y***↓***G***TGLTP	Yalamanchili et al. (1997)
Rhinovirus 14		3Cpro	(AV)XXQ↓G	**NF-κB**	LLN***Q***↓***G***IP	Neznanov et al. (2005)
				eIF5B	***VMEQ***↓***G***	de Breyne et al. (2008)
Echovirus 1		3C		**NF-κB**	LLN***Q***↓***G***IP	Neznanov et al. (2005)
Coxsackie B virus				eIF5B	***VMEQ***↓***G***	de Breyne et al. (2008)
Foot and Mouth disease Virus (FMDV)		3Cpro	(QE)↓(LIGS)	**NEMO**	L*A*LPS***Q***↓RRSPPE	Wang et al. (2012)
				eIF4AI	TN*VRAE*↓VQK*L*QM	Li et al. (2001)
				Histone H3	*P*RK***QL***↓A*TKA*A	Falk et al. (1990)
		Leader protease		eIF4G	SFAN*LG*↓***R***TTLST	Foeger et al. (2002)
Hepatitis A Virus		3Cpro	(LVI)X(TSA)(QEX)↓XXXX	**NEMO**	PV*LKA****Q***↓ADIYK	Wang et al. (2012)
				PABP	A***Q***↓***G***A	Sun et al. (2017)
		3ABC		**MAVS**	*LA****SQ***↓*VD*SP	Yang et al. (2007)
		3CD		**TRIF**	D***WSQ***↓***GC****S*L	Qu et al. (2011)
				TRIF	IREQ***SQ***↓HL*D*G	Qu et al. (2011)
Calicivirus	*Caliciviridae*	3C-like protease	YELQ↓GPE	PABP	VHV***Q***↓***G***QN	Kuyumcu-Martinez et al. (2004a)
Dengue	*Flaviviridae*	ns2B/ns3	QKKKQR↓SGVLWD	**STING (MITA)**	VRACLGCPLR***R***↓GAL*LLL*SIY	Yu et al. (2012)
West Nile Virus		ns2B/ns3		**STING (MITA)**		Ding et al. (2018)
Japanese Encephlitis Virus		ns2B/ns3		**STING (MITA)**		Ding et al. (2018)
Zika Virus		ns2B/ns3	(KG)(KR)R↓(SG)	**STING (MITA)**	HIH***S***RY*R*↓***G***SYWRT*VR*	Ding et al. (2018)
				SFRP1	SEG***GRR***↓***GAALGV****LL*	**(this work)**
				Gs alpha	QV***AGRR***↓***GAAL***PC*SL*	**(this work)**
				NT5M	VP***AGRR***↓***GAA****GGLGL*	**(this work)**
				FOXG1	*KLAFKR*↓***GARL***TSTG	**(this work)**
Hepatitis C Virus		ns3/4A	C↓(SA)	**MAVS**	*E*RE***VPC***↓HRPS	Meylan et al. (2005), Bellecave et al. (2010)
				TRIF	PPPPPS***STPC***↓***S****AHL*TPSSLE	Li et al. (2005a)
VEEV	*Togaviridae*	nsP2	AG(ACR)↓(GAY)	**TRIM14**	DCFA*T*GRH*Y*WEVDV***QEAGA***↓***G***WWVGA	**(this work)**

Junior et al., 2018). Knockdown of FOXG1 was previously shown to decrease its own expression (Vezzali et al., 2016).

The cleavage of human host proteins by viral proteases (Table 1) may reflect a general antagonistic strategy akin to CRISPR/Cas9 and RNAi/RISC (Fig. 8). The cleavage site sequences recognized by viral proteases do not appear to be randomly selected, as the majority of the proteins are involved in generating the innate immune responses. Viral proteases are known to be highly specific and their specificity has often been exploited to remove fusion tags during protein purification. Several groups have shown that viral proteases can cleave host proteins at sites with relatively little sequence identity to the protease cleavage site sequences in the viral polyprotein. The case presented here shows the longest continuous stretch of nine residues that match the subsite tolerances of a viral protease (Table 1). However, it should be noted that there is no requirement for sequence identity; each subsite in the protease has different tolerances for amino acid side chains and substrates only need to satisfy a specific pattern. The use of this mechanism by Group IV (+)ssRNA viruses may be due to the translation of the viral genome which is essentially a mRNA. The production of viral enzymes, including the RNA-dependent RNA polymerase, precedes the production of dsRNA intermediates. Thus, these viral proteases may have an opportunity to short circuit the MAVS signalosome before the intracellular antiviral responses are triggered by dsRNA intermediates (Akhrymuk et al., 2016).

A protein version of CRISPR/Cas9 and RNAi/RISC has not been previously described, but would likely rely on short stretches of homologous host-pathogen protein sequences (SSHHPS) and a protease that cleaves them. By assimilating the relatively short viral protease cleavage sites (generally < 25 residues) to those of antiviral intracellular host proteins, the virus may effectively gain a function without incorporating a significant amount of new genomic material. The strategy used by these viruses compactly embeds another mechanism of IFN-antagonism reliant on the enzymatic activity of the viral protease. Since viruses co-evolve with their hosts, the use and propagation of these host protein sequences in the nonstructural protein cleavage sites may have been evolutionarily advantageous as viral replication often hinges on protease activity and the virus' ability to antagonize the host's antiviral responses. Better suppression of the host's innate immune responses would favor viral replication and could increase the fitness of the virus. Here we observed higher viral titers of VEEV when the nsP2 protease was able to cleave the TRIM14 protein than in the presence of the CA074me nsP2 protease inhibitor (Fig. 4G and H). The antagonism of the host's innate immune responses by the viral protease also suggests that information about the host may be stored in the viral protease cleavage sites (similar to how a CRISPR spacer sequence contains information about the phage that have infected the host). These cleavage site sequences could yield information about the hosts that have or lack protective antiviral mechanisms. For example, the VEEV nsP2 cysteine protease cleavage site was notably absent in equine (Fig. 5). Host-pathogen interactions also can pose a problem in live virus vaccines, mutating the proteases so that they can

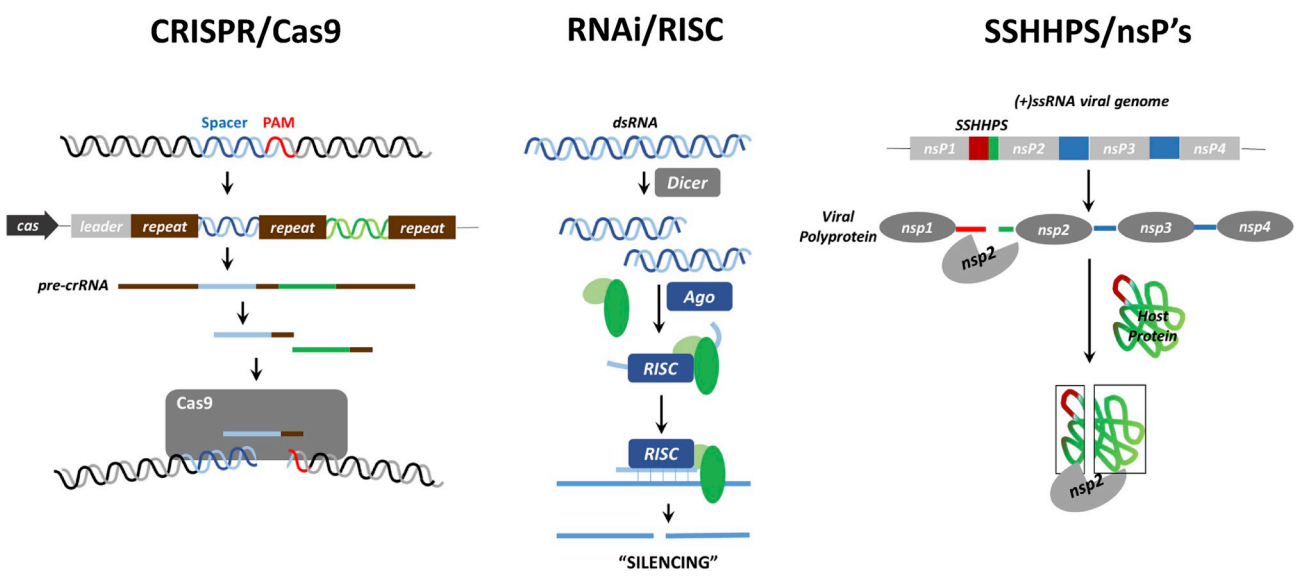

Fig. 8. DNA, RNA, Protein? Three mechanisms of silencing that are guided by a short sequence. In each case a short sequence is used to identify a larger target sequence; these mechanisms are analogous to "search and delete" programs that utilize a "keyword" that have been written in three different languages. Each system has an enzyme that recognizes the match between the short sequence and the target and then cuts ("deletes") the larger target sequence. The short sequence and target sequences belong to either the host or pathogen and the goal of these mechanisms is to antagonize or silence the effects of the molecule. These mechanisms are used to defend the host from viruses or to defend a virus from a host's immune system. The CRISPR/Cas9 and RNAi figures have been adapted from http://parts.igem.org/Collections/CRISPR and http://www.gene-quantification.de/siRNA-mechanism.png.

no longer cleave the host proteins, could be a useful strategy for de-risking a live virus vaccine.

What is common among these three mechanisms of silencing is that they each rely on a short sequence to identify a larger target sequence to destroy; they are analogous to "search and delete" algorithms that utilize a "keyword" to identify a file to delete (Fig. 8). Each of these programs carries an enzyme able to identify a match between the short sequence and the larger target sequence and then cleave the identified target. All of the mechanisms are used to silence or antagonize a response; the relationship between the short sequence and the target sequence is typically between a host and pathogen, more specifically a virus. In each case these mechanisms are used as defensive mechanisms, protecting the host from a virus or a virus from a host.

Modulation of the innate immune responses by small molecules to treat acute viral infections is still a challenging problem in drug discovery. Pathogen-specific mechanisms of innate immune response suppression are of significant interest to ongoing drug discovery efforts against viral encephalitides and Zika since one small molecule may be able to exert two beneficial effects- inhibition of viral replication and alleviation of suppression of the innate immune responses.

Funding

This work was supported by DTRA project numbers CB-SEED-SEED09-2-0061 and CBCall4-CBM-05-2-0019, Office of Naval Research (ONR) 6.1 base funding, and the NRL HBCU/MI summer internship program sponsored by the ONR (#N0017315RMV04).

Acknowledgment

We would like to thank Dr. Jonah Cheung at the New York Structural Biology Center and Dr. Rolf Hilgenfeld and Dr. Jian Lei at the University of Lűbeck, Germany for providing plasmids. We also would like to thank Dr. Natasha Zachara at the Johns Hopkins School of Medicine for helpful discussions and technical advice. The opinions expressed here are those of the authors and do not represent those of the U.S. Army, U. S. Navy, U. S. Department of Defense or any other department or agency of the Federal government.

Appendix A. Supplementary data

Supplementary data to this article can be found online at https://doi.org/10.1016/j.antiviral.2019.02.001.

References

Aguirre, S., Maestre, A.M., Pagni, S., Patel, J.R., Savage, T., Gutman, D., Maringer, K., Bernal-Rubio, D., Shabman, R.S., Simon, V., Rodriguez-Madoz, J.R., Mulder, L.C., Barber, G.N., Fernandez-Sesma, A., 2012. DENV inhibits type I IFN production in infected cells by cleaving human STING. PLoS Pathog. 8 e1002934.

Akhrymuk, I., Kulemzin, S.V., Frolova, E.I., 2012. Evasion of the innate immune response: the Old World alphavirus nsP2 protein induces rapid degradation of Rpb1, a catalytic subunit of RNA polymerase II. J. Virol. 86, 7180–7191.

Akhrymuk, I., Frolov, I., Frolova, E.I., 2016. Both RIG-I and MDA5 detect alphavirus replication in concentration-dependent mode. Virology 487, 230–241.

Altschul, S.F., Gish, W., Miller, W., Myers, E.W., Lipman, D.J., 1990. Basic local alignment search tool. J. Mol. Biol. 215, 403–410.

Alvarez, E., Castello, A., Menendez-Arias, L., Carrasco, L., 2006. HIV protease cleaves poly (A)-binding protein. Biochem. J. 396, 219–226.

Atasheva, S., Fish, A., Fornerod, M., Frolova, E.I., 2010. Venezuelan equine Encephalitis virus capsid protein forms a tetrameric complex with CRM1 and importin alpha/beta that obstructs nuclear pore complex function. J. Virol. 84, 4158–4171.

Augustine, C., Gunnersen, J., Spirkoska, V., Tan, S.S., 2001. Place- and time-dependent expression of mouse sFRP-1 during development of the cerebral neocortex. Mech. Dev. 109, 395–397.

Barral, P.M., Morrison, J.M., Drahos, J., Gupta, P., Sarkar, D., Fisher, P.B., Racaniello, V.R., 2007. MDA-5 is cleaved in poliovirus-infected cells. J. Virol. 81, 3677–3684.

Barral, P.M., Sarkar, D., Fisher, P.B., Racaniello, V.R., 2009. RIG-I is cleaved during picornavirus infection. Virology 391, 171–176.

Bellecave, P., Sarasin-Filipowicz, M., Donze, O., Kennel, A., Gouttenoire, J., Meylan, E., Terracciano, L., Tschopp, J., Sarrazin, C., Berg, T., Moradpour, D., Heim, M.H., 2010. Cleavage of mitochondrial antiviral signaling protein in the liver of patients with chronic hepatitis C correlates with a reduced activation of the endogenous interferon system. Hepatology 51, 1127–1136.

Bhoj, V.G., Sun, Q., Bhoj, E.J., Somers, C., Chen, X., Torres, J.P., Mejias, A., Gomez, A.M., Jafri, H., Ramilo, O., Chen, Z.J., 2008. MAVS and MyD88 are essential for innate immunity but not cytotoxic T lymphocyte response against respiratory syncytial virus. Proc. Natl. Acad. Sci. U. S. A. 105, 14046–14051.

Bieniasz, P.D., 2004. Intrinsic immunity: a front-line defense against viral attack. Nat. Immunol. 5, 1109–1115.

Bodine, P.V., Zhao, W., Kharode, Y.P., Bex, F.J., Lambert, A.J., Goad, M.B., Gaur, T., Stein, G.S., Lian, J.B., Komm, B.S., 2004. The Wnt antagonist secreted frizzled-related protein-1 is a negative regulator of trabecular bone formation in adult mice. Mol. Endocrinol. 18, 1222–1237.

Caires-Junior, L.C., Goulart, E., Melo, U.S., Araujo, B.H.S., Alvizi, L., Soares-Schanoski, A., de Oliveira, D.F., Kobayashi, G.S., Griesi-Oliveira, K., Musso, C.M., Amaral, M.S., daSilva, L.F., Astray, R.M., Suarez-Patino, S.F., Ventini, D.C., Gomes da Silva, S.,

Yamamoto, G.L., Ezquina, S., Naslavsky, M.S., Telles-Silva, K.A., Weinmann, K., van der Linden, V., van der Linden, H., de Oliveira, J.R.M., Arrais, N.M.R., Melo, A., Figueiredo, T., Santos, S., Meira, J.G.C., Passos, S.D., de Almeida, R.P., Bispo, A.J.B., Cavalheiro, E.A., Kalil, J., Cunha-Neto, E., Nakaya, H., Andreata-Santos, R., de Souza Ferreira, L.C., Verjovski-Almeida, S., Ho, P.L., Passos-Bueno, M.R., Zatz, M., 2018. Discordant congenital Zika syndrome twins show differential in vitro viral susceptibility of neural progenitor cells. Nat. Commun. 9, 475.

Campos-Gomez, J., Ahmad, F., Rodriguez, E., Saeed, M.F., 2016. A novel cell-based assay to measure activity of Venezuelan equine encephalitis virus nsP2 protease. Virology 496, 77–89.

Carthagena, L., Bergamaschi, A., Luna, J.M., David, A., Uchil, P.D., Margottin-Goguet, F., Mothes, W., Hazan, U., Transy, C., Pancino, G., Nisole, S., 2009. Human TRIM gene expression in response to interferons. PLoS One 4, e4894.

Chang, J.T., Esumi, N., Moore, K., Li, Y., Zhang, S., Chew, C., Goodman, B., Rattner, A., Moody, S., Stetten, G., Campochiaro, P.A., Zack, D.J., 1999. Cloning and characterization of a secreted frizzled-related protein that is expressed by the retinal pigment epithelium. Hum. Mol. Genet. 8, 575–583.

Cheung, J.F., Mancia, F., Rudolph, M., Cassidy, M., Gary, E., Burshteyn, F., Love, J., 2011. Structure of the Chikungunya Virus nsP2 Protease. RCSB PDB.

Clark, M.E., Hammerle, T., Wimmer, E., Dasgupta, A., 1991. Poliovirus proteinase 3C converts an active form of transcription factor IIIC to an inactive form: a mechanism for inhibition of host cell polymerase III transcription by poliovirus. EMBO J. 10, 2941–2947.

Clark, M.E., Lieberman, P.M., Berk, A.J., Dasgupta, A., 1993. Direct cleavage of human TATA-binding protein by poliovirus protease 3C in vivo and in vitro. Mol. Cell Biol. 13, 1232–1237.

Compton, J.R., Mickey, M.J., Hu, X., Marugan, J.J., Legler, P.M., 2017. Mutation of Asn-475 in the Venezuelan equine encephalitis virus nsP2 cysteine protease leads to a self-inhibited state. Biochemistry 56, 6221–6230.

Cugola, F.R., Fernandes, I.R., Russo, F.B., Freitas, B.C., Dias, J.L., Guimaraes, K.P., Benazzato, C., Almeida, N., Pignatari, G.C., Romero, S., Polonio, C.M., Cunha, I., Freitas, C.L., Brandao, W.N., Rossato, C., Andrade, D.G., Faria Dde, P., Garcez, A.T., Buchpigel, C.A., Braconi, C.T., Mendes, E., Sall, A.A., Zanotto, P.M., Peron, J.P., Muotri, A.R., Beltrao-Braga, P.C., 2016. The Brazilian Zika virus strain causes birth defects in experimental models. Nature 534, 267–271.

D'Cruz, A.A., Babon, J.J., Norton, R.S., Nicola, N.A., Nicholson, S.E., 2013. Structure and function of the SPRY/B30.2 domain proteins involved in innate immunity. Protein Sci. 22, 1–10.

Das, S., Dasgupta, A., 1993. Identification of the cleavage site and determinants required for poliovirus 3CPro-catalyzed cleavage of human TATA-binding transcription factor TBP. J. Virol. 67, 3326–3331.

Dastidar, S.G., Narayanan, S., Stifani, S., D'Mello, S.R., 2012. Transducin-like enhancer of Split-1 (TLE1) combines with Forkhead box protein G1 (FoxG1) to promote neuronal survival. J. Biol. Chem. 287, 14749–14759.

de Breyne, S., Bonderoff, J.M., Chumakov, K.M., Lloyd, R.E., Hellen, C.U., 2008. Cleavage of eukaryotic initiation factor eIF5B by enterovirus 3C proteases. Virology 378, 118–122.

Ding, M.X., Schlesinger, M.J., 1989. Evidence that Sindbis virus NSP2 is an autoprotease which processes the virus nonstructural polyprotein. Virology 171, 280–284.

Ding, Q., Gaska, J.M., Douam, F., Wei, L., Kim, D., Balev, M., Heller, B., Ploss, A., 2018. Species-specific disruption of STING-dependent antiviral cellular defenses by the Zika virus NS2B3 protease. Proc. Natl. Acad. Sci. U. S. A. 115, E6310–E6318.

Esteve, P., Sandonis, A., Cardozo, M., Malapeira, J., Ibanez, C., Crespo, I., Marcos, S., Gonzalez-Garcia, S., Toribio, M.L., Arribas, J., Shimono, A., Guerrero, I., Bovolenta, P., 2011. SFRPs act as negative modulators of ADAM10 to regulate retinal neurogenesis. Nat. Neurosci. 14, 562–569.

Fagerberg, L., Hallstrom, B.M., Oksvold, P., Kampf, C., Djureinovic, D., Odeberg, J., Habuka, M., Tahmasebpoor, S., Danielsson, A., Edlund, K., Asplund, A., Sjostedt, E., Lundberg, E., Szigyarto, C.A., Skogs, M., Takanen, J.O., Berling, H., Tegel, H., Mulder, J., Nilsson, P., Schwenk, J.M., Lindskog, C., Danielsson, F., Mardinoglu, A., Sivertsson, A., von Feilitzen, K., Forsberg, M., Zwahlen, M., Olsson, I., Navani, S., Huss, M., Nielsen, J., Ponten, F., Uhlen, M., 2014. Analysis of the human tissue-specific expression by genome-wide integration of transcriptomics and antibody-based proteomics. Mol. Cell. Proteomics 13, 397–406.

Falk, M.M., Grigera, P.R., Bergmann, I.E., Zibert, A., Multhaup, G., Beck, E., 1990. Foot-and-mouth disease virus protease 3C induces specific proteolytic cleavage of host cell histone H3. J. Virol. 64, 748–756.

Fata, C.L., Sawicki, S.G., Sawicki, D.L., 2002. Alphavirus minus-strand RNA synthesis: identification of a role for Arg183 of the nsP4 polymerase. J. Virol. 76, 8632–8640.

Foeger, N., Glaser, W., Skern, T., 2002. Recognition of eukaryotic initiation factor 4G isoforms by picornaviral proteinases. J. Biol. Chem. 277, 44300–44309.

Fotaki, V., Smith, R., Pratt, T., Price, D.J., 2013. Foxg1 is required to limit the formation of ciliary margin tissue and Wnt/beta-catenin signalling in the developing nasal retina of the mouse. Dev. Biol. 380, 299–313.

Fros, J.J., Pijlman, G.P., 2016. Alphavirus Infection: Host Cell Shut-Off and Inhibition of Antiviral Responses. Viruses 8.

Garmashova, N., Gorchakov, R., Frolova, E., Frolov, I., 2006. Sindbis virus nonstructural protein nsP2 is cytotoxic and inhibits cellular transcription. J. Virol. 80, 5686–5696.

Garmashova, N., Gorchakov, R., Volkova, E., Paessler, S., Frolova, E., Frolov, I., 2007a. The Old World and New World alphaviruses use different virus-specific proteins for induction of transcriptional shutoff. J. Virol. 81, 2472–2484.

Garmashova, N., Atasheva, S., Kang, W., Weaver, S.C., Frolova, E., Frolov, I., 2007b. Analysis of Venezuelan equine encephalitis virus capsid protein function in the inhibition of cellular transcription. J. Virol. 81, 13552–13565.

Goodfellow, F.T., Tesla, B., Simchick, G., Zhao, Q., Hodge, T., Brindley, M.A., Stice, S.L., 2016. Zika virus induced mortality and microcephaly in chicken embryos. Stem Cell. Dev. 25, 1691–1697.

Graham, K.L., Gustin, K.E., Rivera, C., Kuyumcu-Martinez, N.M., Choe, S.S., Lloyd, R.E., Sarnow, P., Utz, P.J., 2004. Proteolytic cleavage of the catalytic subunit of DNA-dependent protein kinase during poliovirus infection. J. Virol. 78, 6313–6321.

Grigera, P.R., Tisminetzky, S.G., 1984. Histone H3 modification in BHK cells infected with foot-and-mouth disease virus. Virology 136, 10–19.

Gropman, A.L., Duncan, W.C., Smith, A.C., 2006. Neurologic and developmental features of the Smith-Magenis syndrome (del 17p11.2). Pediatr. Neurol. 34, 337–350.

Hardy, W.R., Strauss, J.H., 1989. Processing the nonstructural polyproteins of sindbis virus: nonstructural proteinase is in the C-terminal half of nsP2 and functions both in cis and in trans. J. Virol. 63, 4653–4664.

Hirose, S., Nishizumi, H., Sakano, H., 2003. Pub, a novel PU.1 binding protein, regulates the transcriptional activity of PU.1. Biochem. Biophys. Res. Commun. 311, 351–360.

Hiscott, J., Lacoste, J., Lin, R., 2006. Recruitment of an interferon molecular signaling complex to the mitochondrial membrane: disruption by hepatitis C virus NS3-4A protease. Biochem. Pharmacol. 72, 1477–1484.

Hollidge, B.S., Weiss, S.R., Soldan, S.S., 2011. The role of interferon antagonist, non-structural proteins in the pathogenesis and emergence of arboviruses. Viruses 3, 629–658.

Hu, X., Compton, J.R., Leary, D.H., Olson, M.A., Lee, M.S., Cheung, J., Ye, W., Ferrer, M., Southall, N., Jadhav, A., Morazzani, E.M., Glass, P.J., Marugan, J., Legler, P.M., 2016. Kinetic, mutational, and structural studies of the Venezuelan equine encephalitis virus nonstructural protein 2 cysteine protease. Biochemistry 55, 3007–3019.

Hu, G., Pen, W., Wang, M., 2018. TRIM14 promotes breast cancer cell proliferation by inhibiting apoptosis. Oncol. Res. https://doi.org/10.3727/096504018X15214994641786. PMID: 29562956.

Ibrahim, B., McMahon, D.P., Hufsky, F., Beer, M., Deng, L., Mercier, P.L., Palmarini, M., Thiel, V., Marz, M., 2018. A new era of virus bioinformatics. Virus Res. 251, 86–90.

Jacob, F.D., Ramaswamy, V., Andersen, J., Bolduc, F.V., 2009. Atypical Rett syndrome with selective FOXG1 deletion detected by comparative genomic hybridization: case report and review of literature. Eur. J. Hum. Genet. 17, 1577–1581.

James, L.C., Keeble, A.H., Khan, Z., Rhodes, D.A., Trowsdale, J., 2007. Structural basis for PRYSPRY-mediated tripartite motif (TRIM) protein function. Proc. Natl. Acad. Sci. U. S. A. 104, 6200–6205.

Jia, X., Zhou, H., Wu, C., Wu, Q., Ma, S., Wei, C., Cao, Y., Song, J., Zhong, H., Zhou, Z., Wang, J., 2017. The ubiquitin ligase RNF125 targets innate immune adaptor protein TRIM14 for ubiquitination and degradation. J. Immunol. 198, 4652–4658.

Kading, R.C., Schountz, T., 2016. Flavivirus infections of bats: potential role in Zika virus ecology. Am. J. Trop. Med. Hyg. 95, 993–996.

Kiemer, L., Lund, O., Brunak, S., Blom, N., 2004. Coronavirus 3CLpro proteinase cleavage sites: possible relevance to SARS virus pathology. BMC Bioinf. 5, 72.

Kortum, F., Das, S., Flindt, M., Morris-Rosendahl, D.J., Stefanova, I., Goldstein, A., Horn, D., Klopocki, E., Kluger, G., Martin, P., Rauch, A., Roumer, A., Saitta, S., Walsh, L.E., Wieczorek, D., Uyanik, G., Kutsche, K., Dobyns, W.B., 2011. The core FOXG1 syndrome phenotype consists of postnatal microcephaly, severe mental retardation, absent language, dyskinesia, and corpus callosum hypogenesis. J. Med. Genet. 48, 396–406.

Kundu, P., Raychaudhuri, S., Tsai, W., Dasgupta, A., 2005. Shutoff of RNA polymerase II transcription by poliovirus involves 3C protease-mediated cleavage of the TATA-binding protein at an alternative site: incomplete shutoff of transcription interferes with efficient viral replication. J. Virol. 79, 9702–9713.

Kuyumcu-Martinez, N.M., Joachims, M., Lloyd, R.E., 2002. Efficient cleavage of ribosome-associated poly(A)-binding protein by enterovirus 3C protease. J. Virol. 76, 2062–2074.

Kuyumcu-Martinez, M., Belliot, G., Sosnovtsev, S.V., Chang, K.O., Green, K.Y., Lloyd, R.E., 2004a. Calicivirus 3C-like proteinase inhibits cellular translation by cleavage of poly(A)-binding protein. J. Virol. 78, 8172–8182.

Kuyumcu-Martinez, N.M., Van Eden, M.E., Younan, P., Lloyd, R.E., 2004b. Cleavage of poly(A)-binding protein by poliovirus 3C protease inhibits host cell translation: a novel mechanism for host translation shutoff. Mol. Cell Biol. 24, 1779–1790.

Lee, Y.S., Lee, K.A., Yoon, H.B., Yoo, S.A., Park, Y.W., Chung, Y., Kim, W.U., Kang, C.Y., 2012. The Wnt inhibitor secreted Frizzled-Related Protein 1 (sFRP1) promotes human Th17 differentiation. Eur. J. Immunol. 42, 2564–2573.

Lei, J., Hansen, G., Nitsche, C., Klein, C.D., Zhang, L., Hilgenfeld, R., 2016. Crystal structure of Zika virus NS2B-NS3 protease in complex with a boronate inhibitor. Science 353, 503–505.

Li, W., Ross-Smith, N., Proud, C.G., Belsham, G.J., 2001. Cleavage of translation initiation factor 4AI (eIF4AI) but not eIF4AII by foot-and-mouth disease virus 3C protease: identification of the eIF4AI cleavage site. FEBS Lett. 507, 1–5.

Li, K., Foy, E., Ferreon, J.C., Nakamura, M., Ferreon, A.C., Ikeda, M., Ray, S.C., Gale Jr., M., Lemon, S.M., 2005a. Immune evasion by hepatitis C virus NS3/4A protease-mediated cleavage of the Toll-like receptor 3 adaptor protein TRIF. Proc. Natl. Acad. Sci. U. S. A. 102, 2992–2997.

Li, J., Lim, S.P., Beer, D., Patel, V., Wen, D., Tumanut, C., Tully, D.C., Williams, J.A., Jiricek, J., Priestle, J.P., Harris, J.L., Vasudevan, S.G., 2005b. Functional profiling of recombinant NS3 proteases from all four serotypes of dengue virus using tetrapeptide and octapeptide substrate libraries. J. Biol. Chem. 280, 28766–28774.

Liang, Y.L., Khoshouei, M., Radjainia, M., Zhang, Y., Glukhova, A., Tarrasch, J., Thal, D.M., Furness, S.G.B., Christopoulos, G., Coudrat, T., Danev, R., Baumeister, W., Miller, L.J., Christopoulos, A., Kobilka, B.K., Wootten, D., Skiniotis, G., Sexton, P.M., 2017. Phase-plate cryo-EM structure of a class B GPCR-G-protein complex. Nature 546, 118–123.

Lin, R., Lacoste, J., Nakhaei, P., Sun, Q., Yang, L., Paz, S., Wilkinson, P., Julkunen, I., Vitour, D., Meurs, E., Hiscott, J., 2006. Dissociation of a MAVS/IPS-1/VISA/Cardif-IKKepsilon molecular complex from the mitochondrial outer membrane by hepatitis C virus NS3-4A proteolytic cleavage. J. Virol. 80, 6072–6083.

Ma, M., Adams, H.R., Seltzer, L.E., Dobyns, W.B., Paciorkowski, A.R., 2016. Phenotype differentiation of FOXG1 and MECP2 disorders: a new method for characterization of developmental encephalopathies. J. Pediatr. 178, 233–240 e210.
Malim, M.H., Bieniasz, P.D., 2012. HIV restriction factors and mechanisms of evasion. Cold Spring Harb. Perspect Med. 2, a006940.
Marcos, S., Nieto-Lopez, F., Sandonis, A., Cardozo, M.J., Di Marco, F., Esteve, P., Bovolenta, P., 2015. Secreted frizzled related proteins modulate pathfinding and fasciculation of mouse retina ganglion cell axons by direct and indirect mechanisms. J. Neurosci. 35, 4729–4740.
Mariani, J., Coppola, G., Zhang, P., Abyzov, A., Provini, L., Tomasini, L., Amenduni, M., Szekely, A., Palejev, D., Wilson, M., Gerstein, M., Grigorenko, E.L., Chawarska, K., Pelphrey, K.A., Howe, J.R., Vaccarino, F.M., 2015. FOXG1-Dependent dysregulation of GABA/glutamate neuron differentiation in autism spectrum disorders. Cell 162, 375–390.
Meylan, E., Curran, J., Hofmann, K., Moradpour, D., Binder, M., Bartenschlager, R., Tschopp, J., 2005. Cardif is an adaptor protein in the RIG-I antiviral pathway and is targeted by hepatitis C virus. Nature 437, 1167–1172.
Miquelajauregui, A., Van de Putte, T., Polyakov, A., Nityanandam, A., Boppana, S., Seuntjens, E., Karabinos, A., Higashi, Y., Huylebroeck, D., Tarabykin, V., 2007. Smad-interacting protein-1 (Zfhx1b) acts upstream of Wnt signaling in the mouse hippocampus and controls its formation. Proc. Natl. Acad. Sci. U. S. A. 104, 12919–12924.
Morazzani, E.M., Compton, J.R.L., D.H., Zachara, N.E., Hu, X., Marugan, J.J., Glass, P.J.L., P.M, 2017. Proteolytic cleavage of TRIM14 by the VEEV nonstructural protein 2 cysteine protease. In: American Chemical Society. ACS, Washington, D.C BIOL-20.
Morris, G.M., Huey, R., Lindstrom, W., Sanner, M.F., Belew, R.K., Goodsell, D.S., Olson, A.J., 2009. AutoDock4 and AutoDockTools4: automated docking with selective receptor flexibility. J. Comput. Chem. 30, 2785–2791.
Munir, M., 2010. TRIM proteins: another class of viral victims. Sci. Signal. 3, jc2.
Nenasheva, V.V., Kovaleva, G.V., Uryvaev, L.V., Ionova, K.S., Dedova, A.V., Vorkunova, G.K., Chernyshenko, S.V., Khaidarova, N.V., Tarantul, V.Z., 2015. Enhanced expression of trim14 gene suppressed Sindbis virus reproduction and modulated the transcription of a large number of genes of innate immunity. Immunol. Res. 62, 255–262.
Neznanov, N., Chumakov, K.M., Neznanova, L., Almasan, A., Banerjee, A.K., Gudkov, A.V., 2005. Proteolytic cleavage of the p65-RelA subunit of NF-kappaB during poliovirus infection. J. Biol. Chem. 280, 24153–24158.
Nisole, S., Stoye, J.P., Saib, A., 2005. TRIM family proteins: retroviral restriction and antiviral defence. Nat. Rev. Microbiol. 3, 799–808.
Ozato, K., Shin, D.M., Chang, T.H., Morse, H.C., 2008. TRIM family proteins and their emerging roles in innate immunity. Nat. Rev. Immunol. 8, 849–860 3rd.
Parekh, B.S., Maniatis, T., 1999. Virus infection leads to localized hyperacetylation of histones H3 and H4 at the IFN-beta promoter. Mol. Cell 3, 125–129.
Phoo, W.W., Li, Y., Zhang, Z., Lee, M.Y., Loh, Y.R., Tan, Y.B., Ng, E.Y., Lescar, J., Kang, C., Luo, D., 2016. Structure of the NS2B-NS3 protease from Zika virus after self-cleavage. Nat. Commun. 7, 13410.
Pratt, D.W., Warner, J.V., Williams, M.G., 2013. Genotyping FOXG1 mutations in patients with clinical evidence of the FOXG1 syndrome. Mol. Syndromol. 3, 284–287.
Qiao, Y., Kang, K., Giannopoulou, E., Fang, C., Ivashkiv, L.B., 2016. IFN-gamma induces histone 3 lysine 27 trimethylation in a small subset of promoters to stably silence gene expression in human macrophages. Cell Rep. 16, 3121–3129.
Qu, L., Feng, Z., Yamane, D., Liang, Y., Lanford, R.E., Li, K., Lemon, S.M., 2011. Disruption of TLR3 signaling due to cleavage of TRIF by the hepatitis A virus protease-polymerase processing intermediate, 3CD. PLoS Pathog. 7 e1002169.
Rampazzo, C., Gallinaro, L., Milanesi, E., Frigimelica, E., Reichard, P., Bianchi, V., 2000. A deoxyribonucleotidase in mitochondria: involvement in regulation of dNTP pools and possible link to genetic disease. Proc. Natl. Acad. Sci. U. S. A. 97, 8239–8244.
Ratia, K., Pegan, S., Takayama, J., Sleeman, K., Coughlin, M., Baliji, S., Chaudhuri, R., Fu, W., Prabhakar, B.S., Johnson, M.E., Baker, S.C., Ghosh, A.K., Mesecar, A.D., 2008. A noncovalent class of papain-like protease/deubiquitinase inhibitors blocks SARS virus replication. Proc. Natl. Acad. Sci. U. S. A. 105, 16119–16124.
Reagan, R.L., Rumbaugh, H., Nelson, H., Brueckner, A.L., 1955. Effect of zika virus and bwamba virus in the cave bat (myotus lucifugus). Trans. Am. Microsc. Soc. 74, 77–79.
Romero-Brey, I., Bartenschlager, R., 2016. Endoplasmic reticulum: the favorite intracellular niche for viral replication and assembly. Viruses 8.
Ruge, D.R., Dunning, F.M., Piazza, T.M., Molles, B.E., Adler, M., Zeytin, F.N., Tucker, W.C., 2011. Detection of six serotypes of botulinum neurotoxin using fluorogenic reporters. Anal. Biochem. 411, 200–209.
Satoh, W., Gotoh, T., Tsunematsu, Y., Aizawa, S., Shimono, A., 2006. Sfrp1 and Sfrp2 regulate anteroposterior axis elongation and somite segmentation during mouse embryogenesis. Development 133, 989–999.
Schechter, I., Berger, A., 1967. On the size of the active site in proteases. I. Papain. Biochem. Biophys. Res. Commun. 27, 157–162.
Schoggins, J.W., Rice, C.M., 2011. Interferon-stimulated genes and their antiviral effector functions. Curr. Opin. Virol. 1, 519–525.
Shin, G., Yost, S.A., Miller, M.T., Elrod, E.J., Grakoui, A., Marcotrigiano, J., 2012. Structural and functional insights into alphavirus polyprotein processing and pathogenesis. Proc. Natl. Acad. Sci. U. S. A. 109, 16534–16539.
Shiryaev, S.A., Farhy, C., Pinto, A., Huang, C.T., Simonetti, N., Elong Ngono, A., Dewing, A., Shresta, S., Pinkerton, A.B., Cieplak, P., Strongin, A.Y., Terskikh, A.V., 2017. Characterization of the Zika virus two-component NS2B-NS3 protease and structure-assisted identification of allosteric small-molecule antagonists. Antivir. Res. 143, 218–229.
Simmons, J.D., White, L.J., Morrison, T.E., Montgomery, S.A., Whitmore, A.C., Johnston, R.E., Heise, M.T., 2009. Venezuelan equine encephalitis virus disrupts STAT1 signaling by distinct mechanisms independent of host shutoff. J. Virol. 83, 10571–10581.
Smith, J.L., Jeng, S., McWeeney, S.K., Hirsch, A.J., 2017. A MicroRNA screen identifies the Wnt signaling pathway as a regulator of the interferon response during flavivirus infection. J. Virol. 91.
Strauss, E.G., De Groot, R.J., Levinson, R., Strauss, J.H., 1992. Identification of the active site residues in the nsP2 proteinase of Sindbis virus. Virology 191, 932–940.
Su, X., Wang, J., Chen, W., Li, Z., Fu, X., Yang, A., 2016. Overexpression of TRIM14 promotes tongue squamous cell carcinoma aggressiveness by activating the NF-kappaB signaling pathway. Oncotarget 7, 9939–9950.
Sun, D., Wang, M., Wen, X., Cheng, A., Jia, R., Sun, K., Yang, Q., Wu, Y., Zhu, D., Chen, S., Liu, M., Zhao, X., Chen, X., 2017. Cleavage of poly(A)-binding protein by duck hepatitis A virus 3C protease. Sci. Rep. 7, 16261.
Swaroop, A., Agarwal, N., Gruen, J.R., Bick, D., Weissman, S.M., 1991. Differential expression of novel Gs alpha signal transduction protein cDNA species. Nucleic Acids Res. 19, 4725–4729.
Tan, P., He, L., Cui, J., Qian, C., Cao, X., Lin, M., Zhu, Q., Li, Y., Xing, C., Yu, X., Wang, H.Y., Wang, R.F., 2017. Assembly of the WHIP-TRIM14-PPP6C mitochondrial complex promotes RIG-I-mediated antiviral signaling. Mol. Cell 68, 293–307 e295.
Trevant, B., Gaur, T., Hussain, S., Symons, J., Komm, B.S., Bodine, P.V., Stein, G.S., Lian, J.B., 2008. Expression of secreted frizzled related protein 1, a Wnt antagonist, in brain, kidney, and skeleton is dispensable for normal embryonic development. J. Cell. Physiol. 217, 113–126.
Uhlen, M., Fagerberg, L., Hallstrom, B.M., Lindskog, C., Oksvold, P., Mardinoglu, A., Sivertsson, A., Kampf, C., Sjostedt, E., Asplund, A., Olsson, I., Edlund, K., Lundberg, E., Navani, S., Szigyarto, C.A., Odeberg, J., Djureinovic, D., Takanen, J.O., Hober, S., Alm, T., Edqvist, P.H., Berling, H., Tegel, H., Mulder, J., Rockberg, J., Nilsson, P., Schwenk, J.M., Hamsten, M., von Feilitzen, K., Forsberg, M., Persson, L., Johansson, F., Zwahlen, M., von Heijne, G., Nielsen, J., Ponten, F., 2015. Proteomics. Tissue-based map of the human proteome. Science 347, 1260419.
Vezzali, R., Weise, S.C., Hellbach, N., Machado, V., Heidrich, S., Vogel, T., 2016. The FOXG1/FOXO/SMAD network balances proliferation and differentiation of cortical progenitors and activates Kcnh3 expression in mature neurons. Oncotarget 7, 37436–37455.
Wang, D., Fang, L., Li, K., Zhong, H., Fan, J., Ouyang, C., Zhang, H., Duan, E., Luo, R., Zhang, Z., Liu, X., Chen, H., Xiao, S., 2012. Foot-and-mouth disease virus 3C protease cleaves NEMO to impair innate immune signaling. J. Virol. 86, 9311–9322.
Wang, D., Fang, L., Wei, D., Zhang, H., Luo, R., Chen, H., Li, K., Xiao, S., 2014. Hepatitis A virus 3C protease cleaves NEMO to impair induction of beta interferon. J. Virol. 88, 10252–10258.
Wang, S., Chen, Y., Li, C., Wu, Y., Guo, L., Peng, C., Huang, Y., Cheng, G., Qin, F.X., 2016. TRIM14 inhibits hepatitis C virus infection by SPRY domain-dependent targeted degradation of the viral NS5A protein. Sci. Rep. 6, 32336.
Weidman, M.K., Sharma, R., Raychaudhuri, S., Kundu, P., Tsai, W., Dasgupta, A., 2003. The interaction of cytoplasmic RNA viruses with the nucleus. Virus Res. 95, 75–85.
Xu, G., Guo, Y., Xu, D., Wang, Y., Shen, Y., Wang, F., Lv, Y., Song, F., Jiang, D., Zhang, Y., Lou, Y., Meng, Y., Yang, Y., Kang, Y., 2017. TRIM14 regulates cell proliferation and invasion in osteosarcoma via promotion of the AKT signaling pathway. Sci. Rep. 7, 42411.
Yalamanchili, P., Banerjee, R., Dasgupta, A., 1997. Poliovirus-encoded protease 2APro cleaves the TATA-binding protein but does not inhibit host cell RNA polymerase II transcription in vitro. J. Virol. 71, 6881–6886.
Yan, N., Chen, Z.J., 2012. Intrinsic antiviral immunity. Nat. Immunol. 13, 214–222.
Yang, Y., Liang, Y., Qu, L., Chen, Z., Yi, M., Li, K., Lemon, S.M., 2007. Disruption of innate immunity due to mitochondrial targeting of a picornaviral protease precursor. Proc. Natl. Acad. Sci. U. S. A. 104, 7253–7258.
Yu, C.Y., Chang, T.H., Liang, J.J., Chiang, R.L., Lee, Y.L., Liao, C.L., Lin, Y.L., 2012. Dengue virus targets the adaptor protein MITA to subvert host innate immunity. PLoS Pathog. 8 e1002780.
Zhang, Y., Burke, C.W., Ryman, K.D., Klimstra, W.B., 2007. Identification and characterization of interferon-induced proteins that inhibit alphavirus replication. J. Virol. 81, 11246–11255.
Zhang, D., Tozser, J., Waugh, D.S., 2009. Molecular cloning, overproduction, purification and biochemical characterization of the p39 nsp2 protease domains encoded by three alphaviruses. Protein Expr. Purif. 64, 89–97.
Zhou, Z., Jia, X., Xue, Q., Dou, Z., Ma, Y., Zhao, Z., Jiang, Z., He, B., Jin, Q., Wang, J., 2014. TRIM14 is a mitochondrial adaptor that facilitates retinoic acid-inducible gene-I-like receptor-mediated innate immune response. Proc. Natl. Acad. Sci. U. S. A. 111, E245–E254.